(Paper to be submitted to ASME annual meeting.)

INCIDENCE AND DEVIATION ANGLE CORRELATIONS FOR COMPRESSOR CASCADES

By Seymour Lieblein

Lewis Research Center
National Aeronautics and Space Administration
Cleveland, Ohio

ABSTRACT

An analysis is presented for the variation of low-speed minimum-loss incidence angle and deviation angle for compressor cascade blades. The aerodynamics governing the behavior of these angles is discussed, and the principal influencing parameters are established. It is shown that if blade mean camber lines are expressed in terms of an equivalent circular-arc camber line, a single general relation can be obtained for predicting these angles for conventional sections such as the NACA 65-series blades, the British C-series blades, and the double-circular arc blade. The specific constants associated with each blade shape are derived from the available data.

INTRODUCTION

In an earlier paper [1], it was shown that a generalized correlation for the low-speed losses of conventional compressor cascade blades could be obtained when the losses and blade loading were expressed in terms of certain significant parameters. The correlation was obtained for such commonly used blades as the NACA 65(A_{10})-series blades and the British C-4 and C-7 series blades at the reference condition of minimum-loss incidence angle. In view of the success of the loss correlations, it was thought desirable to investigate means of deducing similar generalized correlations for the reference incidence angle and air turning angle variations for these blades. In so doing, a general procedure might be established for predicting the principal performance parameters of conventional cascade blades.

In early cascade investigations, general correlation of air-angle data was made difficult because of the absence of true two-dimensional flow in the cascade tunnels. Nevertheless, several noteworthy attempts [2,3,4,5] were made to correlate limited experimental data for design use. In recent years, however, the introduction of effective tunnel-wall boundary-layer control (notably the porous wall technique developed by the NACA [6]) gave a substantial impetus to cascade analysis. More consistent systematic data [6,7,8] and more significant comparisons between theoretical and experimental performance [9,10,11] were obtained as a result of the improved two-dimensionality. The recent availability of considerable amounts of consistant data has also made feasible further investigation of the general relations among the various cascade flow parameters.

The present paper presents an analysis of the low-speed air turning characteristics of conventional cascade blades in terms of air deviation angle at incidence angle for minimum loss. Available cascade theory and general blade aerodynamics are utilized to obtain a qualitative insight into the behavior of these angles. Empirical correlations are then established based on these considerations to describe the variation of the air angles with cascade geometry and inlet flow conditions. The correlations are expressed in significant parameters applicable to compressor design.

NOMENCLATURE

A	flow area
b	exponent in deviation-angle relation
c	chord length
i	incidence angle, angle between inlet-air direction and tangent to blade mean camber line at leading edge, deg
i_o	incidence angle of uncambered blade section, deg
K_i	correction factor in incidence-angle relation
K_δ	correction factor in deviation-angle relation
M	Mach number
m	slope factor in deviation-angle relation
n	slope factor in incidence-angle relation
s	blade spacing
t	blade maximum thickness
V	air velocity

α angle of attack, angle between inlet-air direction and blade chord, deg

β air angle, angle between air velocity and axial direction, deg

$\Delta\beta$ air turning angle, $\beta_1 - \beta_2$, deg

γ blade-chord angle, angle between blade chord and axial direction, deg

δ deviation angle, angle between outlet-air direction and tangent to blade mean camber line at trailing edge, deg

δ_o deviation angle of uncambered blade section, deg

σ solidity, ratio of chord to spacing

φ blade camber angle, difference between angles of tangents to mean camber line at leading and trailing edges, deg

$\bar{\omega}$ total-pressure-loss coefficient, $\Delta P \Big/ \frac{1}{2}\rho V_1^2$

Subscripts:

l lower surface

ref reference

sh blade shape

t blade maximum thickness

u upper surface

1 station at cascade inlet

2 station at cascade exit (measuring station)

10 10 percent thick

PRELIMINARY CONSIDERATIONS

Blade Designation

Nomenclature and symbols designating cascade blade characteristics are given in figure 1. As in isolated-airfoil practice, cascade blade shapes are normally evolved by adding a basic thickness distribution to a mean camber line which, as indicated in figure 1, represents the basic curvature of the profile. Some frequently used curvatures are the NACA (A_{10}) and related mean lines [6,8], the circular-arc mean line [4], and the parabolic-arc mean line [7]. Two popular basic thickness distributions are the NACA 65-series thickness distribution [6] and the British C.4 thickness distribution [4]. A high-speed profile has also been obtained from the construction of a circular-arc upper and lower surface [12]; this profile is referred to as the double-circular-arc blade.

Data Selection

In view of the sensitivity of cascade air angles to the degree of two-dimensionality attained in the tunnel, data for the basic correlations were selected only from large tunnels or fron tunnels in which good wall boundary-layer control was exercised [e.g., 6,11]. Furthermore, the data were restricted to values of blade-chord Reynolds number from about 2.0×10^5 to 2.5×10^5 in order to minimize possible Reynolds number effects on the loss and angle variations. However, in some cases [e.g., 6,14] in tunnels with low turbulence levels, local laminar-separation effects were observed in the range of Reynolds number selected. In such instances, it was necessary to estimate the probable variation of performance parameters against incidence angle in the absence of the local separation, and use

values obtained from the faired curves for the correlations. The specific sources of data used in the analysis are indicated by the reference listed for the various correlations.

Approach

In order to use a uniform nomenclature and consistent correlation technique for the various blade shapes considered, it was believed best to consider the approach characteristics of the blade in terms of air incidence angle i, the camber characteristics in terms of the camber angle φ, and the air-turning characteristics in terms of the deviation angle δ. As indicated in figure 1, these angles are based on the tangents to the blade mean camber line at the leading and trailing edges. The use of the deviation angle, rather than the turning angle, as a measure of the air outlet direction has the advantage, for correlation purposes, of a generally small variation with incidence angle. Air-turning angle is related to the chamber, incidence, and deviation angles by

$$\Delta\beta = \varphi + i - \delta \tag{1}$$

Incidence angle is considered positive when it tends to increase the air-turning angle, and deviation angle is considered positive when it tends to decrease the air-turning angle.

The use of incidence and deviation angles requires a unique and reasonable definition of the blade mean-line angle at the leading and trailing edges, which may not be possible for some blade shapes. The principal difficulty in this respect is in the 65-(A_{10})-series blades [6] whose mean-line slope is theoretically infinite at the leading and trailing edges. However, it is still possible to render these sections usable in the

analysis by arbitrarily establishing an equivalent circular-arc mean camber line. As shown in figure 2, the equivalent circular-arc mean line is obtained by drawing a circular arc through the leading- and trailing-edge points and the point of maximum camber at the midchord position. Equivalent incidence, deviation, and camber angles can then be established from the equivalent circular-arc mean line as indicated in the figure. The relation between equivalent camber angle and isolated-airfoil lift coefficient of the NACA 65-(A_{10})-series mean line is shown in figure 3.

Inasmuch as cascade performance curves vary appreciably with increasing inlet Mach number, it was necessary to restrict the analysis of the low-speed air angles to some reference point on the loss-against-incidence angle curve that exhibits the least variation in magnitude of performance parameters as Mach number is increased. The reference location selected herein is the incidence angle at minimum total-pressure loss, defined specifically as the midpoint of the range of incidence angle between the points of twice minimum loss. Typical variations of total-pressure loss and deviation angle are shown in figure 4.

At this point, it should be kept in mind that the reference minimum-loss incidence angle is not necessarily to be considered as a recommended design point for compressor application. The selection of the best incidence angle for a particular blade element in a multistage-compressor design is a function of many considerations, such as the location of the blade row, the design Mach number, and the type and application of the design. In general, there is no one univeral definition of design or best incidence angle. The cascade reference location is established primarily for purposes of analysis.

Of the many blade shapes currently in use in compressor design practice (i.e., NACA 65-series, C-series circular arc, parabolic arc, double circular arc), data sufficient to permit a reasonably complete and significant correlation have been published only for the 65-(A_{10})-series blades of [6]. Therefore, a basic correlation of the 65-(A_{10})-series data had to be established first and the results used as a guide or foundation for determining the corresponding performance trends for the other blade shapes for which only limited data exist. Accordingly, it was necessary to establish the angle correlations on the basis of fixed air inlet angle rather than fixed chord angle as in the case of the compressor. Limited data indicate that a fixed β_1 curve will have a minimum-loss incidence angle about 1^o to 2^o greater than a fixed γ curve for the same values of β_1 in the low-loss region. An approximate allowance for this difference was made in the correlations when using data from these two procedures.

INCIDENCE-ANGLE VARIATIONS

Qualitative Analysis

It is generally recognized that the low-loss region of incidence angle is identified with the absence of large velocity peaks (and subsequent decelerations) on either blade surface. For infinitely thin sections, steep velocity gradients are avoided when the front stagnation point is located at the leading edge. This condition has frequently been referred to as the condition of "impact-free entry." Weinig [15] used the criterion of stagnation-point location to establish the variation of "impact-free-entry" incidence angle for infinitely thin circular-arc sections from potential-flow theory. Results deduced therein showed that the minimum-loss incidence

angle is zero at zero camber and decreases linearly with camber for fixed solidity and blade-chord angle.

Some equivalent results have been obtained for thick-nose blades with rounded leading edges based on the criterion that the location of the stagnation point in the leading-edge region of a thick blade is the controlling factor in the determination of the surface velocity distributions. Carter [16] showed semitheoretically on this basis that optimum incidence angle (angle at maximum lift-drag ratio) for a conventional 10-percent-thick circular-arc blade decreases with increasing camber angle. These results were followed [17] by generalized plots of the variation of optimum incidence angle for a 10-percent-thick C-series blade with camber angle, solidity, and blade orientation. (In these references, blade orientation was expressed in terms of air outlet angle rather than blade-chord angle.) Apparently, the greater the blade circulation, the lower in magnitude the minimum-loss incidence angle must be. It is reasonable to expect, therefore, that the trends of variation of minimum-loss incidence angle for conventional blade sections will be similar to those established by thin-airfoil theory.

The results of [17] as well as a preliminary examination of experimental cascade data showed that the minimum-loss incidence angles of uncambered sections ($\varphi' = 0$) of conventional thicknesses were not zero, as indicated by theory for infinitely thin blades, but always positive in value. The appearance of positive values of incidence angle for thick blades is attributed to the existence of velocity distributions at zero incidence angle that are not symmetrical on the two surfaces. Apparently, an increase in

incidence angle from the zero value is necessary in order to reduce the lower-surface velocity to a more equitable distribution that results in a minimum of the over-all loss. This zero-camber thickness effect will appear only for blade-chord angles between 0° and 90°, since, as indicated by the highly simplified one-dimensional model of the blade passage flow in figure 5, the velocity distributions at these limit angles are symmetrical. The effect of such a blade thickness blockage on "impact-free-entry" incidence angle for straight (uncambered) blades of constant chordwise thickness in incompressible two-dimensional flow was investigated in [18]. The results showed that, in terms of the parameters used in this paper, the "impact-free" incidence angle is zero at $\beta_1 = 0$, increases with increasing β_1 until a maximum value is reached and then decreases to zero again at $\beta_1 = 90^{\circ}$. It is reasonable to expect that similar trends of variations of zero-camber reference minimum-loss incidence angle will be obtained for compressor blade profiles.

On the basis of the preceding analysis, therefore, it is expected that, for low-speed-cascade flow, reference minimum-loss incidence angle will generally be positive at zero camber and decrease with increasing camber, depending on solidity and blade-chord angle. The available theory also indicates that the variation of reference incidence angle with camber at fixed solidity and chord angle might be essentially linear. If so, the variations could be expressed in terms of slope and intercept values, where the intercept value represents the magnitude of the incidence angle for the uncambered section (function of blade thickness, solidity, and blade-chord angle).

Data Correlations

Form of correlation. - Although preliminary theory indicates that blade-chord angle is the significant blade orientation parameter, it was necessary to establish the data correlations in terms of inlet-air angle, as mentioned previously. The observed cascade data were found to be represented satisfactorily by a linear variation of reference incidence angle with camber angle for fixed solidity and inlet-air angle. The variation of reference minimum-loss incidence angle can then be described in equation for as

$$i = i_o + n\varphi \tag{2}$$

where i_o is the incidence angle for zero camber, and n is the slope of the incidence-angle variation with camber $(i - i_o)/\varphi$.

Since the existence of a finite blade thickness is apparently the cause of the positive values of i_o, it is reasonable to assume that both the magnitude of the maximum thickness and the thickness distribution contribute to the effect. Therefore, since the 10-percent-thick 65-series blades of [6] are to be used as the basis for a generalized correlation of all conventional blade shapes, it is proposed that the zero-camber reference incidence angle be expressed in the form

$$i_o = (K_i)_{sh}(K_i)_t(i_o)_{10} \tag{3}$$

where $(i_o)_{10}$ represents the variation of zero-camber incidence angle for the 10-percent-thick 65-series thickness distribution, $(K_i)_t$ represents any correction necessary for maximum blade thicknesses other than 10 percent, and $(K_i)_{sh}$ represents any correction necessary for a blade shape with a thickness distribution different from that of the 65-series blades.

(For a 10-percent-thick 65-series blade, $(K_i)_t = 1$ and $(K_i)_{sh} = 1$.) The problem, therefore, is reduced to finding the values of n and i_o (through eq. (3)) as functions of the pertinent variables involved for the various blade profiles considered.

NACA 65-(A_{10})-series blades. - From the extensive low-speed-cascade data for the 65-(A_{10})-series blades [6], when expressed in terms of equivalent incidence and camber angles (figs. 2 and 3), plots of i_o and n can be deduced that adequately represented the minimum-loss-incidence-angle variations of the data. The deduced values of i_o and n as functions of solidity and inlet-air angle are given for these blades in figures 6 and 7. Values of intercept i_o and slope n were obtained by fitting a straight line to each data plot of reference incidence angle against camber angle for a fixed solidity and air inlet angle. The straight lines were selected so that both a satisfactory representation of the variation of the data points and a consistent variation of the resulting n and i_o values were obtained.

The deduced rule values and the observed data points compared in figure 8 indicate the effectiveness of the deduced representation. In several configurations, particularly for low cambers, the range of equivalent incidence angle covered in the tests was insufficient to permit an accurate determination of a minimum-loss value. Some of the scatter of the data may be due to the effects of local laminar separation in altering the range characteristics of the sections.

Although the cascade data of [6] include values of inlet-air angle from 30° to 70° and values of solidity from 0.5 to 1.5, the deduced variations in figures 6 and 7 are extrapolated to cover wider ranges of β_1 and

σ. The extrapolation of i_o to zero at $\beta_1 = 0$ is obvious. According to theory [15] however, the value of the slope terms does not vanish at $\beta_1 = 0$. In figure 7, therefore, an arbitrary fairing of the curves down to nonzero values of n was adopted as indicated. Actually, it is not particularly critical to determine the exact value of the slope term at $\beta_1 = 0$ necessary to locate the reference incidence angle precisely, since, for such cases (inlet guide vanes and turbine nozzles), a wide low-loss range of operation is usually obtained. The solidity extrapolations were attempted because of the uniform variations of the data with solidity. However, caution should be exercised in any further extrapolation of the deduced variations.

C-Series circular-arc blades. - The various thickness distributions used in combination with the circular-arc mean line have been designated C.1, C.2, C.3, and so forth [17,19,20]. In general, the various C-series thickness distributions are fairly similar, and have their maximum thickness located at between 30 and 40 percent of the chord length. The 65-series and two of the more popular C-series thickness distributions (C.1 and C.4) are compared on an exaggerated scale in figure 9. (The 65-series profile shown is usually thickened near the trailing edge in actual blade construction.)

In view of the somewhat greater thickness blockage in the forward portions of the C-series blades (fig. 9), it may be that the minimum-loss incidence angles for zero camber for the C-series blades are somewhat greater than those for the 65-series profiles; that is, $(K_i)_{sh} > 1$. In the absence of any definitive cascade data, the value of $(K_i)_{sh}$ for the C-series profiles was arbitrarily taken to be 1.1. Observed minimum-loss incidence angles for an uncambered 10-percent-thick C.4 profile (obtained

from [21]) compared favorably with values predicted from the deduced $(i_o)_{10}$ values for the 65-series blade (fig. 6 and eq. (3)) with an assumed value of $(K_i)_{sh} = 1.1$.

In view of the similarity between the 65-(A_{10})-series mean line and a true circular arc (fig. 2), the applicability of the slope values in figure 7 to the circular-arc mean line was investigated. For the recent cascade data obtained from tunnels having good boundary-layer control [10,13], a check calculation for the 10-percent-thick C.4 circular-arc blades using figures 6 and 7 with $(K_i)_{sh} = 1.1$ revealed good results. For the three configurations in [13] tested at constant $\beta_1(\varphi = 30^\circ)$, the agreement between observed and predicted minimum-loss incidence angles was within 1°. For the one configuration in [10] tested at constant γ $(\varphi = 31^\circ)$, the predicted value of minimum-loss incidence angle was 1.7° greater than the observed value. However, in view of the general 1° to 2° difference between fixed β_1 and fixed γ operation, such a discrepancy is to be expected. On the basis of these limited data, it appears that the low-speed minimum-loss incidence angles for the C-series circular-arc blade can be obtained from the i_o and n values of the 65-series blade with $(K_i)_{sh} = 1.1$

Double-circular-arc blades. - The double-circular-arc blade is composed of circular-arc upper and lower surfaces. The arc for each surface is drawn between the point of maximum thickness at midchord and the tangent to the circles of the leading- and trailing-edge radii. The chordwise thickness distribution for the double-circular-arc profile with 1-percent leading- and trailing-edge edge radius is shown in figure 9. Lack of cascade data again prevents an accurate determination of a reference-

incidence-angle rule for the double circular arc. Since the double-circular-arc blade is thinner than the 65-series blade in the inlet region, the zero-camber incidence angles for the double-circular-arc blade should be somewhat different from those of the 65-series section, with perhaps $(K_i)_{sh} \leq 1$. It can also be assumed, as before, that the slope-term values of figure 7 are valid for the double-circular-arc blade. From an examination of the available cascade data for the double-circular-arc blade ($\varphi = 25^\circ$, $\sigma = 1.333$ [12]; and $\varphi = 40^\circ$, $\sigma = 1.064$ [19], it appears that the use of figures 7 and 8 with a value of $(K_i)_{sh} = 0.7$ in equations (2) and (3) results in a satisfactory comparison between predicted and observed values of reference incidence angle.

Effect of blade maximum thickness. - As indicated previously, some correction (expressed here in terms of $(K_i)_t$, eq. (3)) of the base values of $(i_o)_{10}$ obtained from the 10-percent-thick 65-series blades in figure 6 should exist for other values of blade maximum-thickness ratio. According to the theory of the zero-camber effect, $(K_i)_t$ should be zero for zero thickness and increase as maximum blade thickness is increased, with a value of 1.0 for a thickness ratio of 0.10. Although the very limited low-speed data obtained from blades of variable thickness ratio [22,23] were not completely definitive, it was possible to establish a preliminary thickness-correction factor for reference zero-camber incidence angle as indicated in figure 11 for use in conjunction with equation (3).

Effect of inlet Mach number. - The previous correlations of reference minimum-loss incidence angle have all been based on low-speed-cascade data. It appears from limited high-speed data, however, that minimum-loss incidence angle will vary with increasing inlet Mach number for certain

blade shapes. The variations of minimum-loss incidence angle with inlet Mach number are plotted for several blade shapes in figure 13. The extension of the test data points to lower values of inlet Mach number could not generally be made because of reduced Reynolds numbers or insufficient points to establish the reference location at the lower Mach numbers. In some instances, however, it was possible to obtain low-speed values of incidence angle from other sources.

The blades of figure 13(a) show essentially no variation of minimum-loss incidence angle with inlet Mach number, at least up to a Mach number of about 0.8. The blades of figure 13(b), however, evidence a marked increase in incidence angle with Mach number. Since the most obvious difference between the blades in figures 13(a) and (b) is the construction of the leading-edge region, the data suggest that blades with thick-nose inlet regions tend to show, for the range of inlet Mach number covered, essentially no Mach number effect on minimum loss incidence angle, while blades with sharp leading edges will have a significant Mach number effect. The available data, however, are too limited to conclusively confirm this observation at this time. Furthermore, for the blades that do show a Mach number effect, the magnitude of the variation of reference incidence angle with Mach number is not currently predictable.

DEVIATION-ANGLE VARIATIONS

Qualitative Analysis

Inasmuch as the flow deviation is an expression of the guidance capacity of the passage formed by adjacent blades, it is expected that the cascade geometry (camber, thickness, solidity, and chord angle) will be the principal

influencing factor involved. Cascade potential-flow theory indicates that the deviation angle should increase with blade camber and chord angle and decrease with solidity. Weinig [15] for example, shows that the deviation angle varies linearly with camber for a given value of solidity and chord angle for infinitesimally thin blades at zero incidence. Furthermore, with deviation angle equal to zero at zero camber angle in this theory, it was possible to express the deviation angle as a ratio of the camber angle. Values of the ratio of deviation angle to camber angle for an infinitely thin circular-arc blade of small camber were found to decrease with solidity and increase with chord angle. These values are for the incidence angle for "impact-free entry" previously mentioned, which corresponds essentially to the condition of minimum loss.

The results of [15] indicate that for a blade of zero thickness, the minimum-loss deviation angle is zero at zero camber angle. Analysis indicates, however, that this is not the case for blades of conventional thicknesses. A recent theoretical demonstration of the existence of a positive value of zero-camber deviation angle according to potential-flow calculations is given by Schlichting [11] for a conventional 10-percent-thick profile at zero incidence angle.

It will be recalled from the discussion of the zero-camber minimum-loss incidence angle that, for the conventional staggered cascade ($0^\circ < \gamma < 90^\circ$) with nonzero blade thickness set at zero incidence angle, a greater magnitude of velocity occurs on the blade lower (concave) surface than on the upper (convex) surface. Such velocity distributions result in a negative blade circulation and consequently in a positive deviation angle.

Furthermore, since the deviation angle increases slightly with increasing incidence angle ($d\delta/di$ is positive in potential cascade flow), positive values of deviation angle will likewise be obtained at the condition of minimum-loss incidence angle. Since the zero-camber deviation angle arises from essentially a thickness blockage effect, the characteristics of the variation of minimum-loss zero-camber deviation angle with cascade geometry would be expected to roughly parallel the variation of the minimum-loss zero-camber incidence angle in figure 6. The low-speed reference-deviation-angle correlations may, therefore, involve intercept and slope values as in the case of the reference-incidence-angle correlations.

Data Correlations

Form of correlation. - Examination of deviation-angle data at reference incidence angle reveals that the observed data can be satisfactorily represented by a linear variation of reference deviation angle with camber angle for fixed solidity and air inlet angle. The variation of reference deviation angle can then be expressed in equation form as

$$\delta = \delta_o + m\varphi \tag{4}$$

where δ_o is the reference deviation angle for zero camber and m is the slope of the deviation-angle variation with camber $(\delta - \delta_o)/\varphi$. Furthermore, it was found that the slope term m could be expressed as a function of solidity, so that equation (4) could be expressed as

$$\frac{\delta - \delta_o}{\varphi} = \frac{m_{\sigma=1}}{\sigma^b} \tag{5}$$

were $m_{\sigma=1}$ represents the value of m at a solidity of 1 and b is the solidity exponent (variable with air inlet angle). It will be noted that

equation (5) is similar in form to the frequently used deviation-angle rule for circular-arc blades originally established by Constant [2] and later modified by Carter [24]. Carter's rule for the condition of nominal incidence angle is given by

$$\frac{\delta}{\varphi} = \frac{m_c}{\sqrt{\sigma}} \tag{6}$$

in which m_c is a function of blade-chord angle [24].

As in the case for the zero-camber reference minimum-loss incidence angle, the zero-camber deviation angle can be represented as a function of blade thickness as

$$\delta_o = (K_\delta)_{sh}(K_\delta)_t(\delta_o)_{10} \tag{7}$$

where $(\delta_o)_{10}$ represents the basic variation for the 10-percent-thick 65-series thickness distribution, $(K_\delta)_{sh}$ represents any correction necessary for a blade shape with a thickness distribution different from that of the 65-series blade, and $(K_\delta)_t$ represents any correction necessary for maximum blade thicknesses other than 10 percent. (For a 10-percent-thick 65-series blade, $(K_\delta)_t$ and $(K_\delta)_{sh}$ are equal to 1.) The problem, therefore, is reduced to finding the values of m, b, and δ_o as functions of the pertinent variables involved for the various blade shapes considered.

NACA 65-(A_{10})-series blades. - Values of the intercept term δ_o and the slope term m were obtained by fitting a straight line to each data plot of reference equivalent deviation angle against equivalent camber angle for a fixed solidity and air inlet angle. The straight lines were selected so that both a satisfactory representation of the variation of the data points and a consistent variation for the resulting δ_o and m

values were obtained. The extrapolation of the values of m to $\beta_1 = 0$ was guided by the data for the 65-$(12A_{10})10$ blade at solidities of 1 to 1.5 reported in the cascade guide-vane investigation of [25] (for an aspect ratio of 1, as in [6]).

For the deviation-angle rule given by equation (5), deduced values of $m_{\sigma=1}$ and exponent b as functions of inlet-air angle are presented in figures 13 and 14. The deduced rule values (eq. (5)) and the observed data points are compared in figure 15 to indicate the effectiveness of the deduced representations. The flagged symbols in the high-camber range in the figure represent blade configurations for which marked boundary-layer separation is indicated (equivalent diffusion ratios are greater than about 2 [1]). In view of the higher loss levels for this condition, an increase in the magnitude of the deviation angle is to be expected compared with the values extrapolated from the smaller cambers for which a lower loss level existed.

C-Series circular-arc blades. - In view of the absence of systematic cascade data for the C-series circular-arc blade, an accurate determination of the rule constants cannot be made for this blade shape. However, it was possible to deduce preliminary relations for δ_o and $m_{\sigma=1}$ on the basis of the limited data available. First, it appears that for the uncambered C.4 section of [7,21], if a value of $(K_\delta)_{sh}$ equal to 1.1 (as for the determination of i_o) is used, a satisfactory comparison between predicted and observed δ_o values is obtained. Secondly, several values of the characteristic number $m_{\sigma=1}$ were determined from the cascade data for a C.4 circular-arc profile obtained from tunnels with good boundary-layer control [10,13]

for a solidity of 1.0 and $\beta_1 = 30^\circ$, 42.5°, 45°, and 60°. Values of $(\delta - \delta_0)/\varphi$ were computed for these blades according to the δ_0 variations of figure 12. A value of $m_{\sigma=1}$ for $\beta_1 = 0^\circ$ was obtained from the performance data of a free-stream circular arc inlet guide vane presented in [26]. These values of m are plotted in figure 13 against inlet-air angle, and the proposed variation of $m_{\sigma=1}$ for the circular-arc mean line is shown by the solid line.

In the absence of data covering a range of solidities, it was assumed that the solidity exponent b in the deviation-angle rule of equation (5) is effectively independent of the profile shape and will therefore also be applicable for the circular-arc mean line. This assumption is in agreement with limited experimental data on inlet guide vanes. The variation of ratio of deviation angle to camber angle obtained from constant-thickness circular-arc guide-vane sections of [27] ($\delta_0 = 0^\circ$ for guide vanes) over a wide range of solidities is shown in figure 16. A computated variation based on values of b and $m_{\sigma=1}$ obtained from figures 14 and 13, respectively, is shown in the figure by the solid line.

Double-circular-arc blades. - Although limited data are available for the double-circular-arc blade [12,19], it was felt that these data could not be reliably utilized in the construction of a deviation-angle rule because of the questionable two-dimensionality of the respective test tunnels. However, since the C-series and the double-circular-arc blades differ only in thickness distribution, it is reasonable to expect that, as in the case of the reference-incidence-angle correlations, only the zero-camber deviation angles will be materially affected. Therefore, the $m_{\sigma=1}$ and b values

deduced for the C-series circular-arc blade might also be used for the double-circular-arc blade, but the δ_o values may be different. An arbitrarily selected value of 0.7 for $(K_\delta)_{sh}$ in equation (7) (as for the reference-incidence-angle determination) is suggested for the double-circular-arc blade.

Comparison of rules. - In view of the widespread use of Carter's rule (eq. (6)) for predicting the deviation angle of circular-arc-mean-line blades, some results obtained from the use of Carter's rule were compared with the deduced rule of equation (5). The principal difference between the two rules occurs in the blade orientation parameter used for the m variation and in the δ_o and b variations. The value of the solidity exponent of 1/2 in equation (6) was originally obtained from limited data. Carter, in a later work, [16] proposes a variable solidity exponent and indicates values close to 1 for accelerating cascades and close to 1/2 for decelerating cascades. The variation of b obtained from the NACA 65-(A_{10})-series blades as equivalent circular arcs in figure 14 essentially confirms this trend. Actually, the deviation-angle rule in the form of equation (5) constitutes a modification of Carter's rule.

In addition to the basic differences between the rules in the magnitudes of the m, b, and δ_o values, it is noted that Carter's rule was originally developed for the condition of nominal incidence angle, whereas the modified rule pertains to the reference minimum-loss incidence angle. However, since Carter's rule has frequently been used over a wide range of reference angle in its application, both rules were evaluated, for simplicity, for the reference minimum-loss incidence angle.

An illustrative comparison of predicted reference deviation angle as obtained from Carter's rule and the modified rule for a 10-percent-thick, thick-nosed circular-arc blade is shown by the calculated results in figure 17 for ranges of camber angle, solidity, and inlet-air angle. (Deviation angles in fig. 17 were restricted to cascade configurations producing values of equivalent diffusion ratio less than 2.0 [1].) The plots of figure 17 show that, in practically all cases, the deviation angles given by the modified rule are somewhat greater in magnitude than those predicted by Carter's rule for the 10-percent-thick blade. This is particularly true for the high inlet-air angles. Thus, greater camber angles are required for a given turning angle according to the modified rule. Differences are even less for the double-circular-arc blade, as indicated in figure 18, since the δ_0 values are smaller for these blades. However, it should be kept in mind that the magnitude of the factors in the modified rule are proposed values based on limited data. Further research is required to establish the modified rule on a firmer foundation.

Effect of blade maximum thickness. - A correction factor for the effect of varying maximum thickness ratio on $(\delta_0)_{10}((K_\delta)_t$ in eq. (7)) was deduced from the data for the 65-$(12A_{10})$ blade in [22]. The correction factor was obtained from faired curves of equivalent δ against maximum thickness ratio. Values of δ at $t/c = 0$ for the plots were computed by subtracting the value of $(\delta_0)_{10}$ obtained from figure 12 from the measured values of δ at the 10-percent maximum thickness point. In the absence of further data, it is proposed that this correction curve is also applicable to other conventional blade shapes.

Effect of inlet Mach number. - Experimental variations of minimum-loss deviation angle with inlet Mach number are presented in figure 20 for a thin-nose and a conventional thick-nose circular-arc blade. In contrast to the inlet Mach number effect on minimum-loss incidence angle (fig. 11), little different is observed between the two variations of deviation angle. Actually, variations in Mach number can affect deviation angle in several ways: by changing the blade circulation, the surface boundary-layer development, or the outlet to inlet axial velocity ratio (compressibility effect on the product of density and axial velocity). Apparently, in both cases, the net effect is small in the Mach number range considered.

Variation with incidence angle. - Thus far, of necessity, the analysis has been conducted for flow conditions at only one reference position on the general curve of loss against incidence angle. Ultimately, of course, it is desired to predict flow variations over the entire range of incidence angle. The variation of deviation angle with incidence angle for a fixed geometry in the two-dimensional cascade is primarily a function of the change in the guidance capacity of the cascade arising from the change in orientation of the approaching flow (a potential-flow effect) and from the variation in the wake loss. Since no information is currently available on the effect of losses, attention is centered on deviation-angle variations in the region of low loss, where the trend of variation approaches that of the potential flow.

Examination of potential-flow theory (Weinig, [15], e.g.) shows that a positive slope of deviation angle against incidence angle exists (i.e., deviation angle increases with incidence angle). Calculations based on

theory of Weinig reveal that the magnitude of the slope varies with solidity and blade-chord angle. The deviation-angle slope approaches zero for infinite solidity (deviation angle is essentially constant at high solidity) and increases as solidity is reduced. At constant solidity, the slope of deviation angle against incidence angle increases as the chord angle is increased. These trends indicate physically that the greater the initial guidance effect (high solidity and low blade angle), the less sensitive the deviation angle is tc changes in incidence angle.

For analysis purposes, since the region of low loss is generally small, the variation of deviation angle with incidence angle for a given cascade geometry in the region of minimum loss can be represented as

$$\delta = \delta_{ref} + (i - i_{ref})\left(\frac{d\delta}{di}\right)_{ref} \tag{8}$$

where $(d\delta/di)_{ref}$ represents the slope of the deviation-angle variation at the reference incidence angle. An empirical determination of the magnitude of the slope of the variation of deviation angle with incidence angle was obtained from an analysis of the low-speed experimental data for the 65-(A_{10})10 blades [6]. From the plot of deviation angle against incidence angle for each configuration (as in fig. 4, e.g.), the slope of the curve at the minimum-loss incidence angle was evaluated graphically. The deduced variation of reference slope magnitude $d\delta/di$ obtained from fairings of these values is presented in figure 21 as a function of solidity and inlet-air angle. Qualitative agreement with theory is strongly indicated by the data. Inasmuch as the phenomenon is essentially a guidance or channel effect, it is anticipated that the slope values of figure 21 will also be

applicable for other conventional blade shapes. Thus, it is possible to predict the deviation angle at incidence angles other than the reference location within the low-loss range of operation from the use of equation (8) and figure 21 for constant β_1 operation.

SUMMARY

The foregoing analysis has presented a correlation of experimental air angles for conventional compressor blade sections as obtained in the low-speed two-dimensional cascade. Simple general rules were evolved for the prediction of incidence angle and deviation angle at the reference condition of minimum loss. These results, in conjunction with the loss correlations of [1], can permit an analytical prediction of the complete low-loss-region performance of conventional blades over a wide range of cascade geometries. Such relations can be used to evaluate different stage design diagrams or, conversely, to determine the blade camber and cascade geometry necessary to produce a given velocity triangle and loss level. The rules may also be of help in facilitating comparisons with actual compressor performance.

However, the present analysis is incomplete. Many areas, such as the deviation-angle rule for the double-circular-arc blade, require further data to substantiate the correlations. It is likewise desirable to obtain a better evaluation of the differences between constant inlet-air angle operation and constant chord-angle operation. Furthermore, additional information concerning the influence of high Mach number and off-design incidence angles of cascade performance is needed.

Finally, it is recognized that the performance of a given blade geometry in the compressor configuration will differ from the performance established in the two-dimensional cascade. These differences result from the effects of the various three-dimensional phenomena that occur in compressor blade rows. It is believed, however, that a firm foundation in two-dimensional-cascade flow constitutes an important step toward the complete understanding of the compressor flow. The extent to which cascade-flow performance can be successfully utilized in compressor design can only be established from further comparative evaluations.

REFERENCES

1. Lieblein, S.: Loss and Stall Analysis of Compressor Cascades. Paper No. 58-A-91, ASME, 1958.

2. Constant, H.: Note on Performance of Cascades of Aerofoils. Note No. E.3696, British R.A.E., 1939.

3. Davis, Hunt: A Method of Correlating Axial-Flow-Compressor Cascade Data. A.S.M.E., Trans., vol. 70, no. 8, Nov. 1948, pp. 951-955.

4. Howell, A. R.: The Present Basis of Axial Flow Compressor Design. Pt. I - Cascade Theory and Performance. R. & M. No. 2095, British A.R.C., June 1942.

5. Howell, A. R., and Carter, A. D. S.: Fluid Flow Through Cascades of Aerofoils. Rep. No. R.6, British N.G.T.E., Sept. 1946.
Note: Paper for the 5th International Congress for Applied Mechanics.

6. Herrig, L. Joseph, Emery, James C., and Erwin, John R.: Systematic Two-Dimensional Cascade Tests of NACA 65-Series Compressor Blades at Low Speeds. NACA RM L51G31, 1951.

7. Fletcher, P. J.: Low Speed Tests on Compressor Cascades of Parabolic Cambered Aerofoils. Pt. II - Pitch/Chord Ratio = 0.75. Memo. No. M.159, British N.G.T.E., Nov. 1952.

8. Erwin, John R., Savage, Melvyn, and Emery, James C.: Two-Dimensional Low-Speed Cascade Investigation of NACA Compressor Blade Sections Having a Systematic Variation in Mean-Line Loading. NACA RM L53I30b, 1953.

9. Katzoff, S., and Hannah, Margery E.: Further Comparisons of Theoretical and Experimental Lift and Pressure Distributions on Airfoils in Cascade at Low-Subsonic Speed. NACA TN 2391, 1951.

10. Blight, F. G., and Howard, W.: Tests on Four Airfoil Cascades. Pt. I - Deflection, Drag, and Velocity Distribution. Rep. E.74, Dept. Supply, Aero. Res. Lab., Melbourne (Australia), July 1952.

11. Schlichting, Herman: Problems and Results of Investigations on Cascade Flow. Jour. Aero. Sci., vo. 21, no. 3, Mar. 1954, pp. 163-178.

12. Andrews, S. J.: Tests Related to the Effect of Profile Shape and Camber Line on Compressor Cascade Performance. Rep. No. R.60, British N.G.T.E., Oct. 1949. later issued as ARC R+M 2743

13. Felix, A. Richard, and Emery, James C.: A Comparison of Typical National Gas Turbine Establishment and NACA Axial-Flow Compressor Blade Sections in Cascade at Low Speed. NACA RM L53B26a, 1953.

14. Korbacher, G. K.: A Test on a Compressor Cascade of Aerofoils Having Their Position of Maximum Thickness 40% of the Chord from the Leading Edge and a Pitch/Chord Ratio of 0.75. Memo. No. M.89, British N.G.T.E., June 1950.

15. Weinig, Fritz: The Flow Around the Blades of Turbomachines. Johann Ambrosium Barth (Leipzig), 1935.

16. Carter, A. D.S.: The Low Speed Performance of Related Aerofoils in Cascade. Rep. No. R.55, British N.G.T.E., Sept. 1949. (See also C.P. No. 29, British M.O.S., Sept. 1949.)

17. Jeffs, R. A., Hounsell, A. F., and Adams, R. G.: Further Performance Data for Aerofoils Having C.1, C.2, or C.4 Base Profiles on Circular Arc Camber Lines. Memo. No. M.139, British N.G.T.E., Dec. 1951.

18. Stanitz, John D.: Effect of Blade-Thickness Taper on Axial-Velocity Distribution at the Leading Edge of an Entrance Rotor-Blade Row with Axial Inlet, and the Influence of This Distribution on Alinement of the Rotor Blade for Zero Angle of Attack. NACA TN 2986, 1953.

19. Howell, A. R.: A Note on Compressor Base Aerofoils C.1, C.2, C.3, C.4, C.5, and Aerofoils Made Up of Circular Arcs. Memo. No. M.1011, Power Jets (Res. and Dev.), Ltd., Sept. 1944.

20. Hughes, Hazel P.: Base Profiles C.7. Memo. M.1210, British N.G.T.E., May 1946.

21. Fletcher, P. J.: Low-Speed Tests on Compressor Cascades of Parabolic Cambered Aerofoils. Pt. I - Pitch/Chord Ratio = 1.0. Memo. No. M.81, British N.G.T.E., Mar. 1950.

22. Herrig, L. Joseph, Emery, James C., and Erwin, John R.: Effect of Section Thickness and Trailing-Edge Radius on the Performance of NACA 65-Series Compressor Blades in Cascade at Low Speeds. NACA RM L51J16, 1951.

23. Bailey, W., and Jefferson, J. L.: Compressibility Effects on Cascades of Low Cambered Compressor Blades. Rep. No. E.3972, British R.A.E., May 1943.

24. Carter, A. D. S., and Hughes, Hazel P.: A Theoretical Investigation into the Effect of Profile Shape on the Performance of Aerofoils in Cascade. R. & M. No. 2384, British A.R.C., Mar. 1946.

25. Dunavant, James C.: Cascade Investigation of a Related Series of 6-Percent-Thick Guide-Vane Profiles and Design Charts. NACA RM L54I02, 1954.

26. Alsworth, Charles C., and Iura, Toru: Theoretical and Experimental Investigations of Axial Flow Compressors. Pt. 3 - Progress Report on Loss Measurements in Vortex Blading. Mech. Eng. Lab., C.I.T., July 1951. (Navy Contract N6-ORI-102, Task Order IV.)

27. Mankuta, Harry, and Guentert, Donald C.: Some Effects of Solidity on Turning Through Constant-Thickness Circular-Arc Guide Vanes in Axial Annular Flow. NACA RM E51E07, 1951.

28. Korbacher, G. K.: A Test on a Compressor Cascade of Aerofoils Having Their Position of Maximum Thickness 40% of the Chord and a Position of Maximum Camber of 45% of the Chord from the Leading Edge. Memo. No. M.80, British N.G.T.E., Mar. 1950.

29. Todd, K. W.: An Experimental Study of Three-Dimensional High-Speed Air Conditions in a Cascade of Axial-Flow Compressor Blades. R. & M. No. 2792, British A.R.C., Oct. 1949.

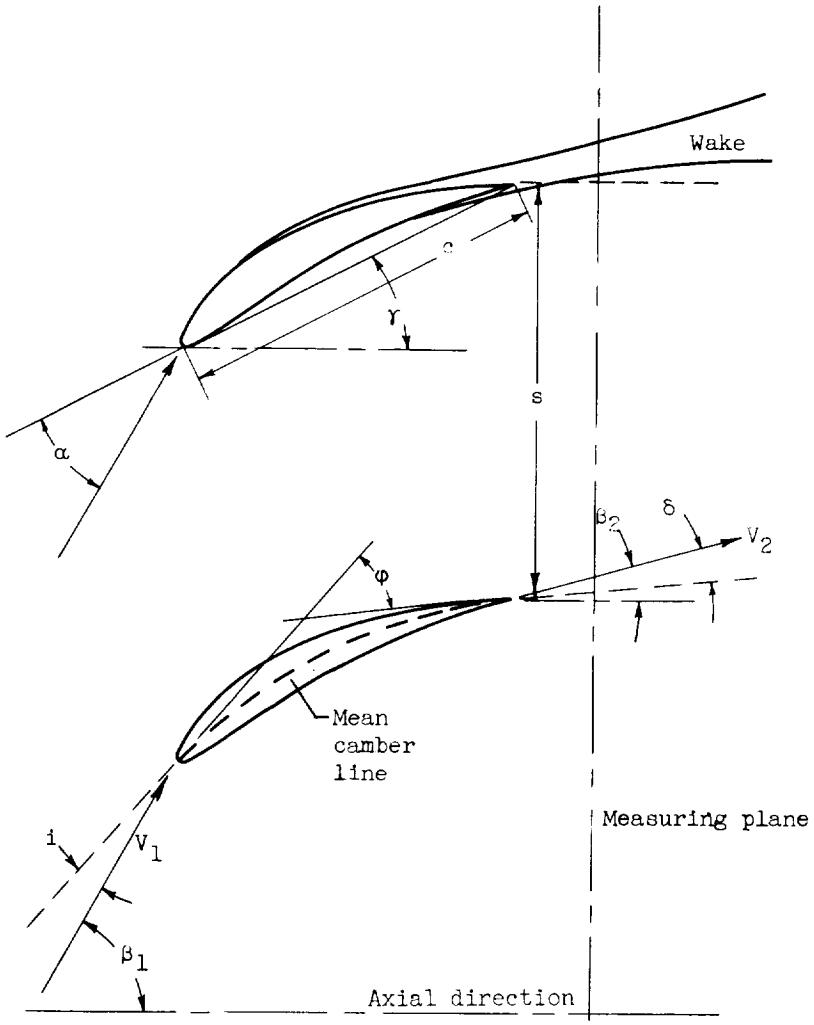

Figure 1. - Nomenclature for cascade blade.

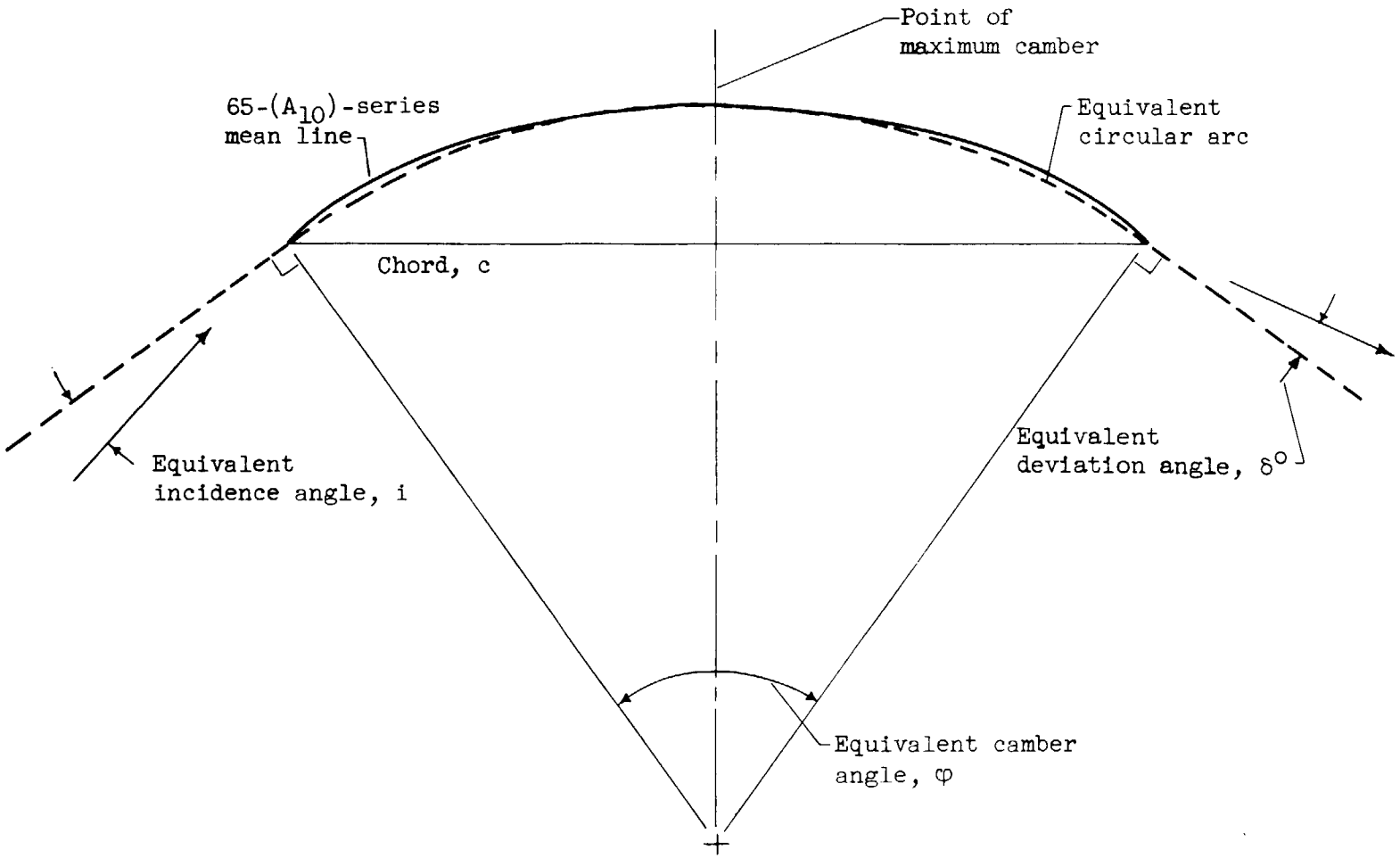

Figure 2. - **Equivalent circular-arc mean line for NACA** 65-(A_{10})-series blades.

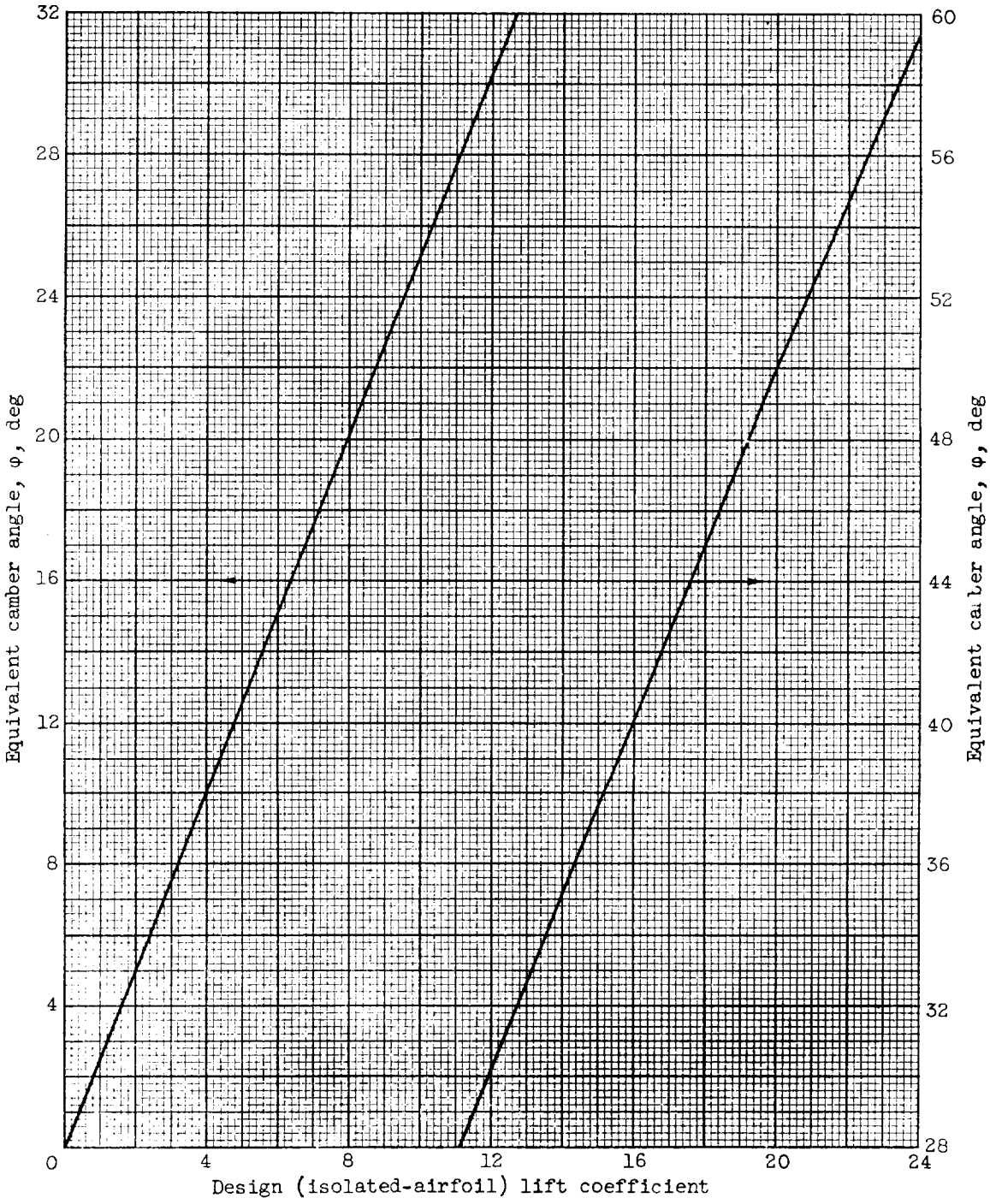

Figure 3. - Equivalent camber angles for NACA 65-($C_{l_o}A_{10}$) mean camber line as equivalent circular arc (fig. 2).

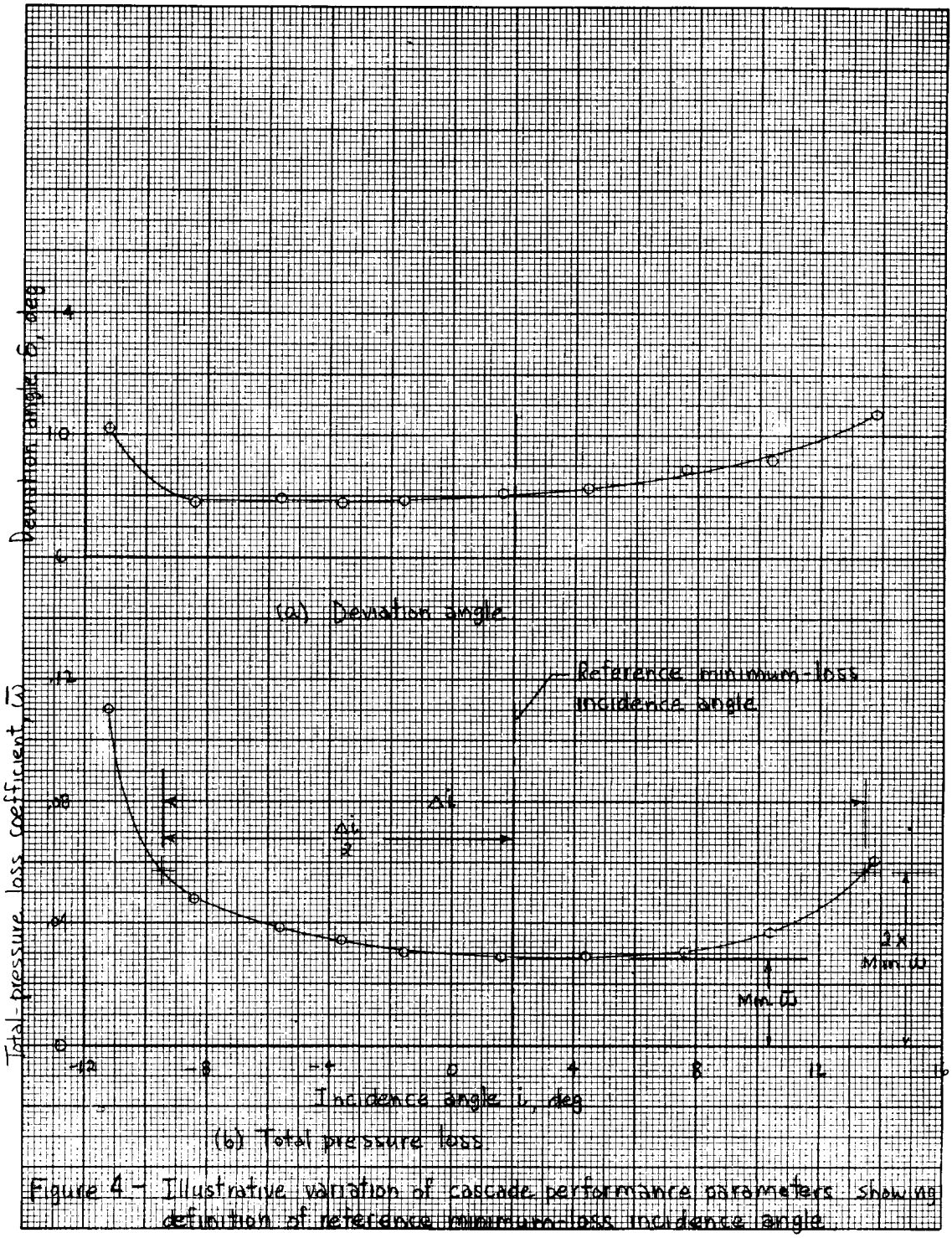

Figure 4 - Illustrative variation of cascade performance parameters showing definition of reference minimum-loss incidence angle.

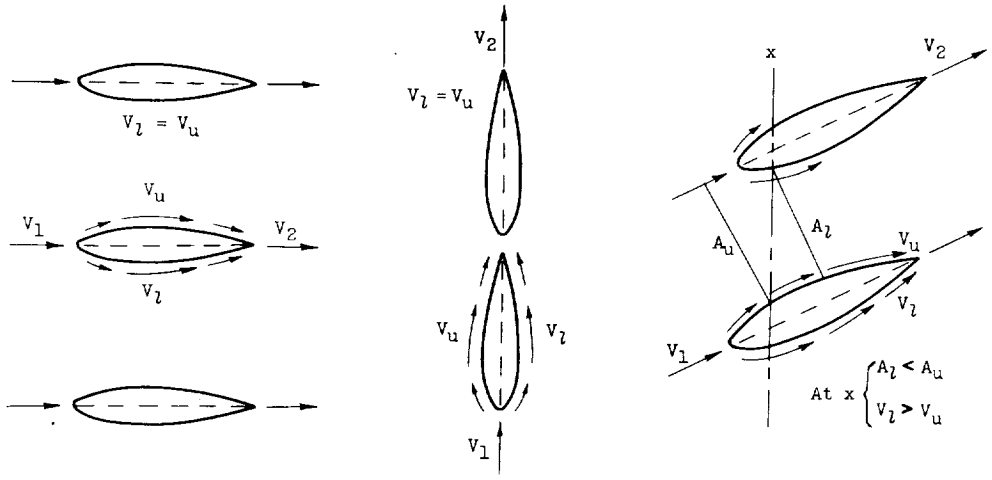

(a) $\gamma^\circ = 0^\circ$. (b) $\gamma^\circ = 90^\circ$. (c) $0^\circ < \gamma^\circ < 90^\circ$.

Figure 5. - Effect of blade thickness on surface velocity at zero incidence angle for uncambered airfoil section according to simplified one-dimensional model.

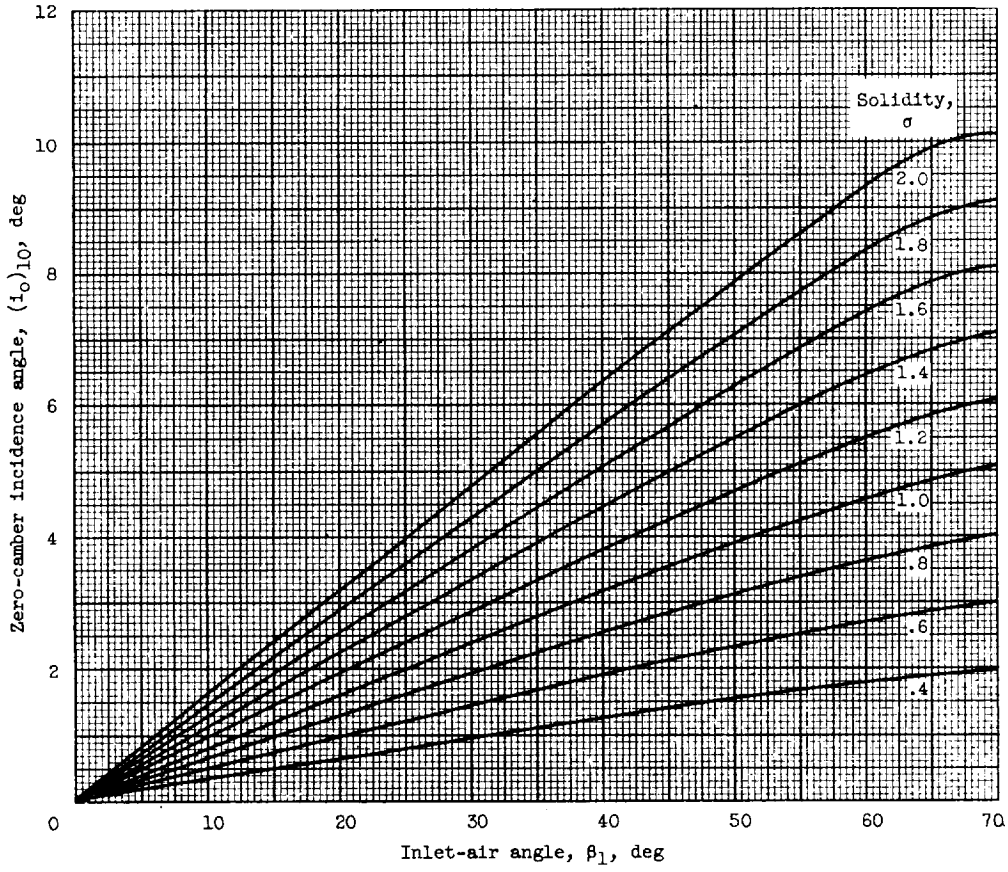

Figure 6. - Reference minimum-loss incidence angle for zero camber deduced from low-speed-cascade data of 10-percent-thick NACA 65-(A_{10})-series blades [6].

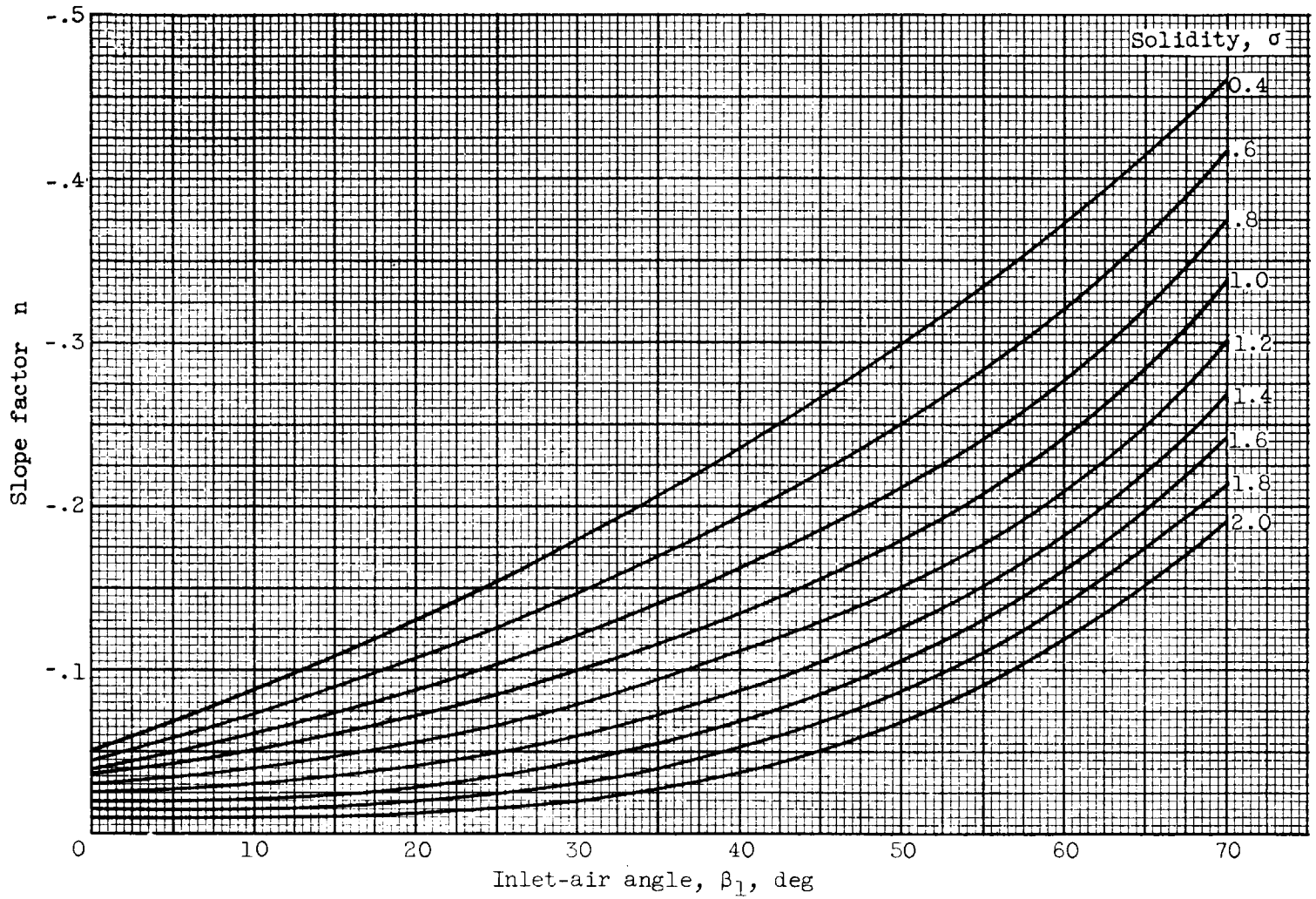

Figure 7. - Reference minimum-loss-incidence-angle slope factor deduced from low-speed-cascade data for NACA 65-(A_{10})-series blades as equivalent circular arcs.

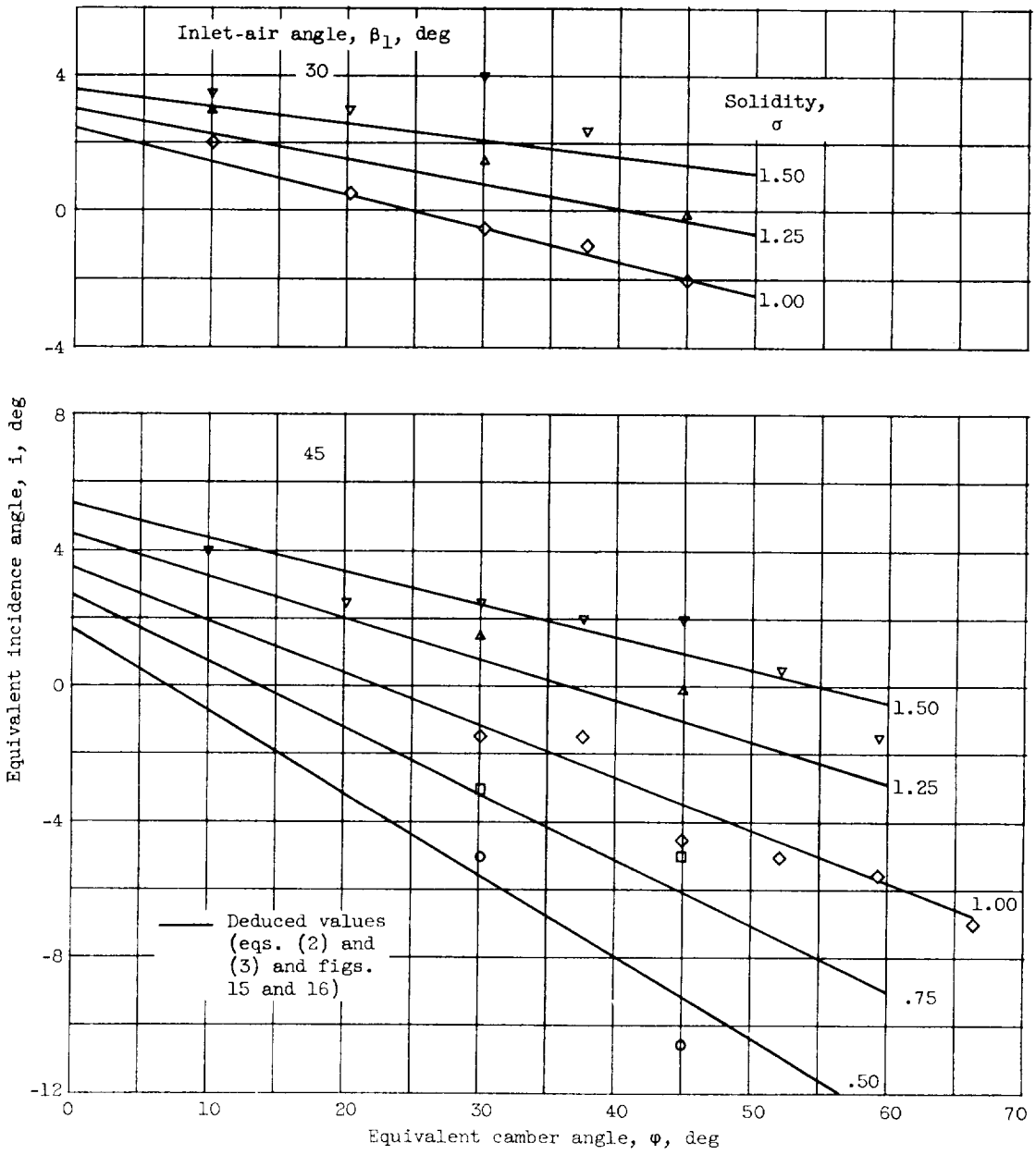

(a) Inlet-air angles of 30° and 45°.

Figure 8. - Comparison of data values and deduced rule values of reference minimum loss incidence angle for 65-(A_{10})10 blades [6] as equivalent circular arcs.

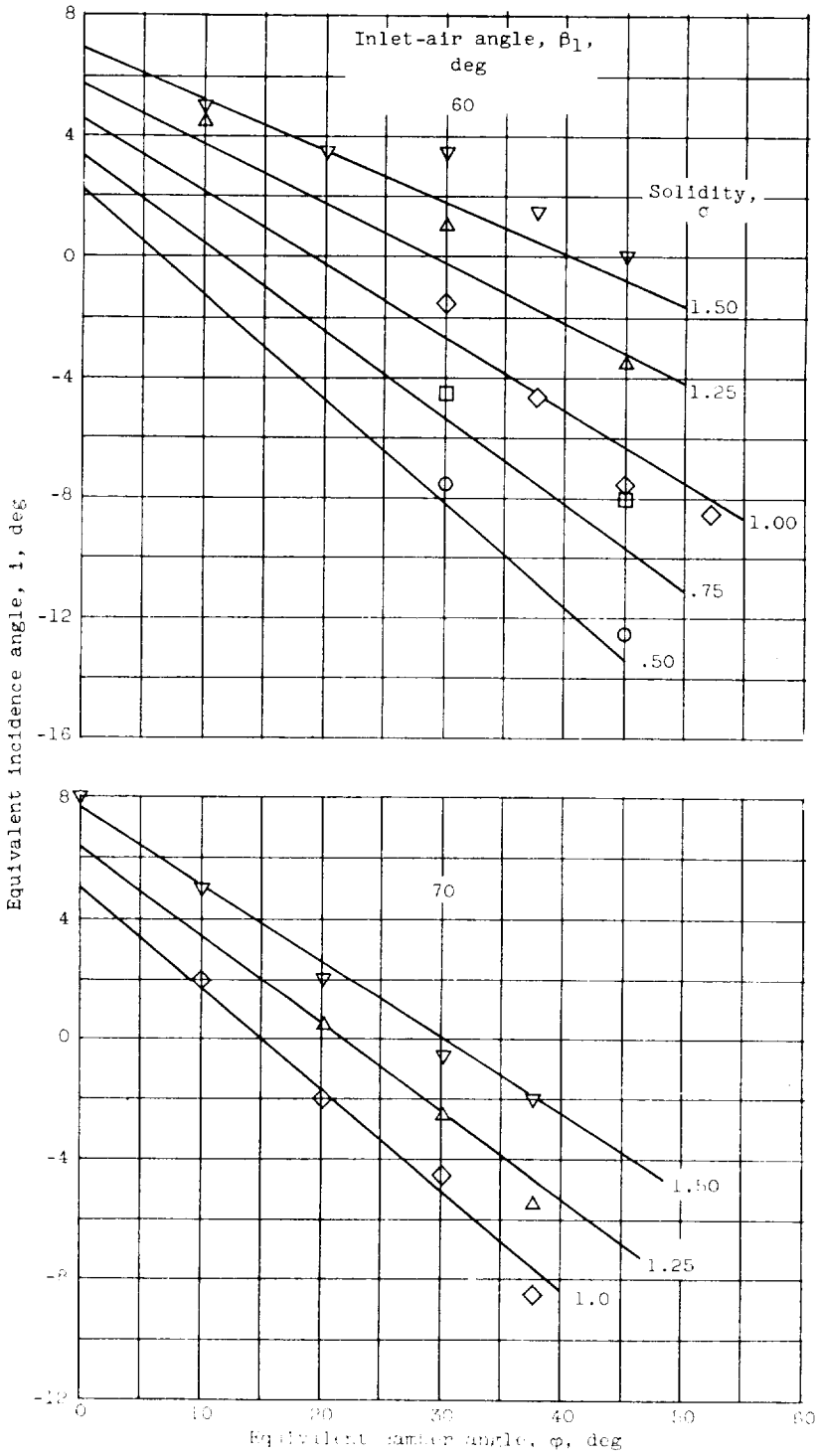

(b) Inlet-air angles of 60° and 70°.

Figure 8. - Concluded. Comparison of data values and deduced rule values of reference minimum loss incidence angle for 65-(A_{10})10 blades [6] equivalent circular arcs.

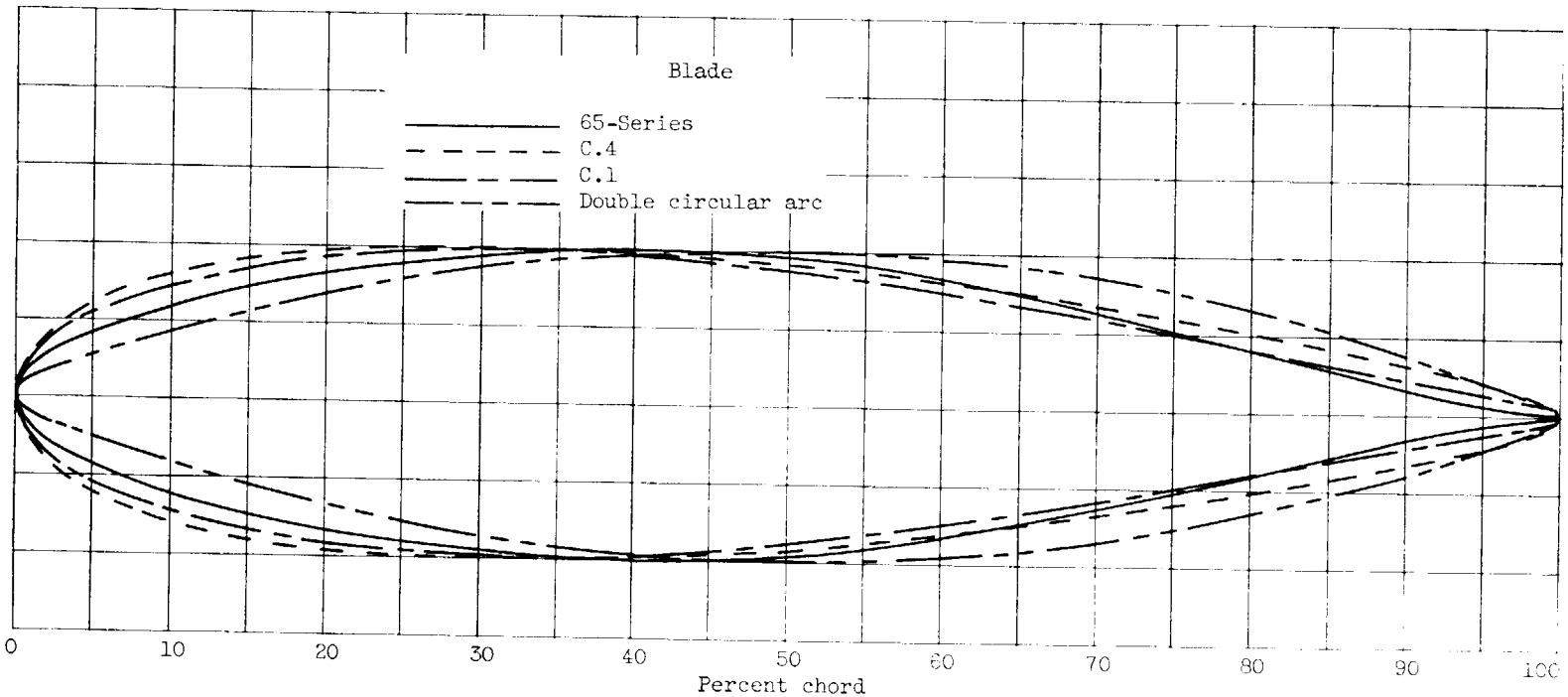

Figure 9. - Comparison of basic thickness distributions for conventional compressor blade sections.

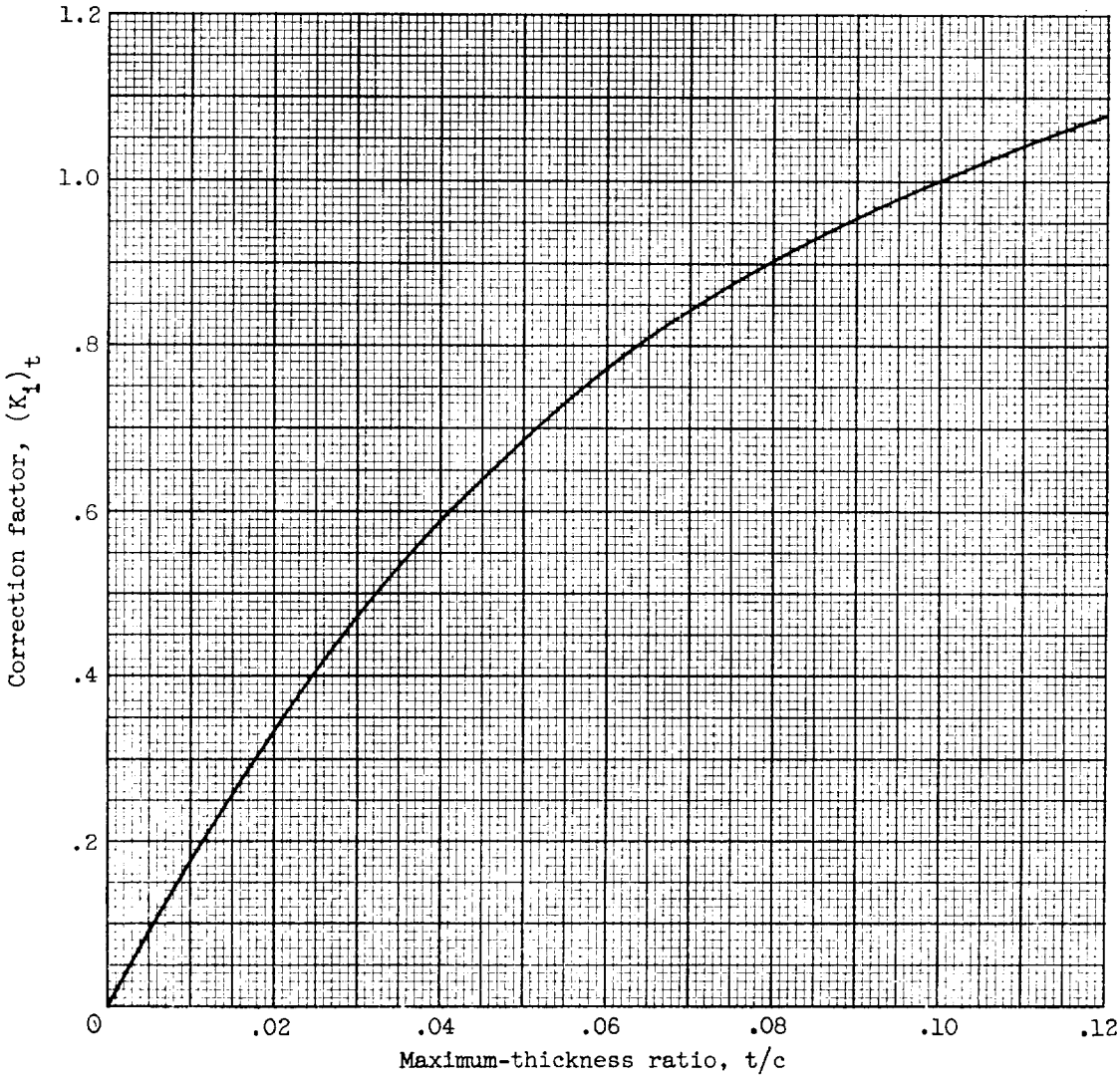

Figure 10. - Deduced blade maximum-thickness correction for zero-camber reference minimum-loss incidence angle (eq. (3)).

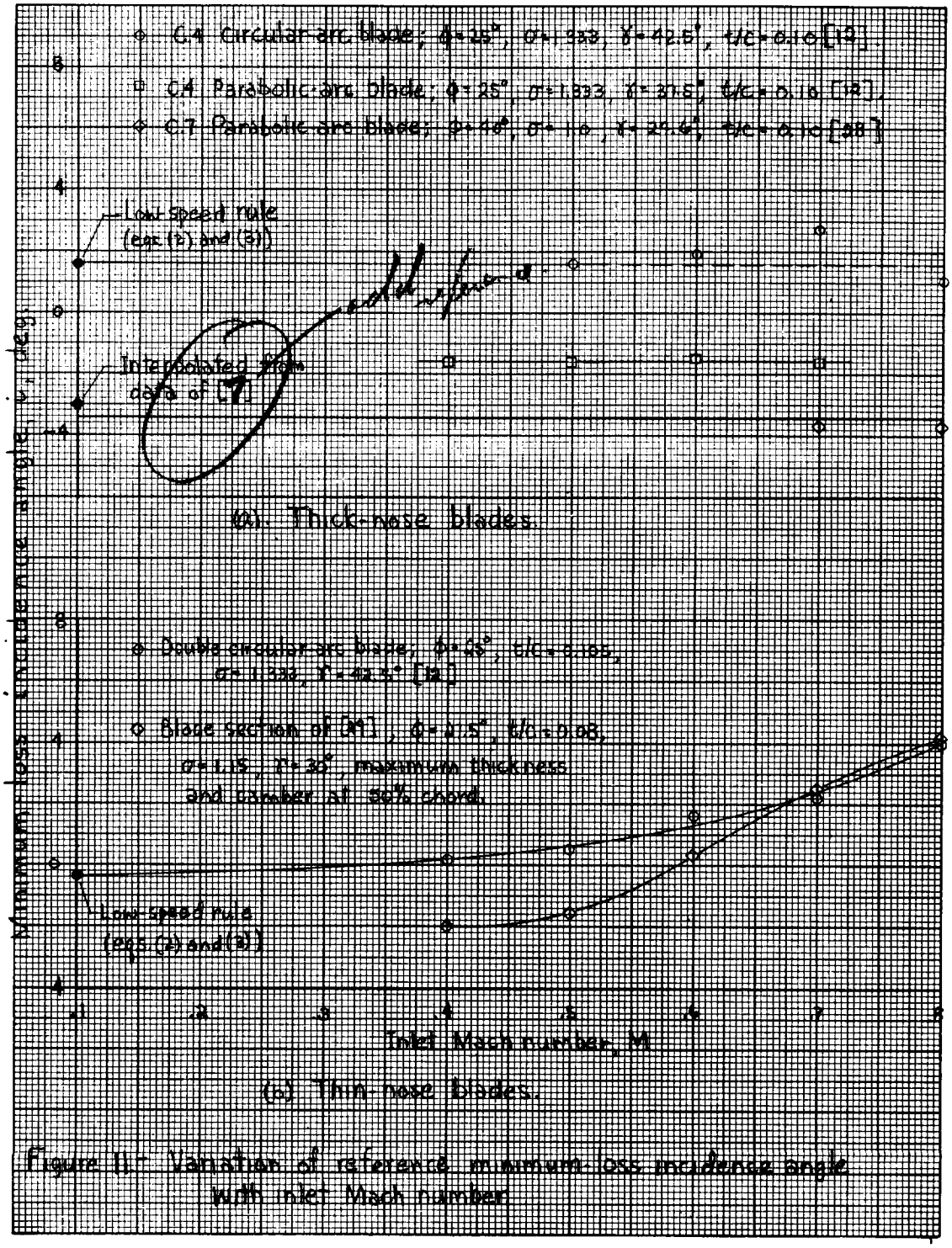

Figure 11.- Variation of referenced minimum-loss incidence angle with inlet Mach number.

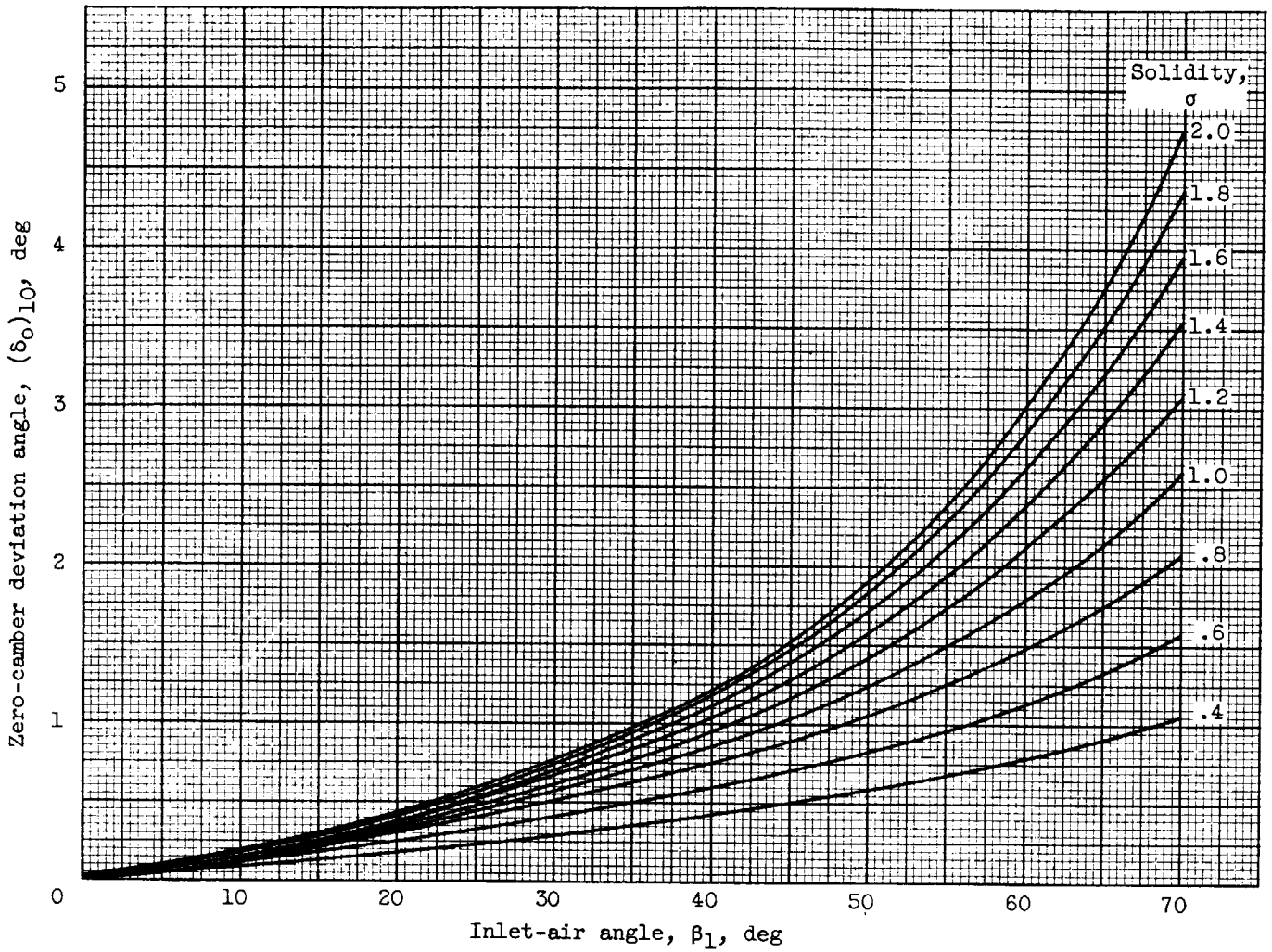

Figure 12. - Zero-camber deviation angle at reference minimum-loss incidence angle deduced from low-speed-cascade data for 10-percent-thick NACA 65-(A_{10})-series blades.

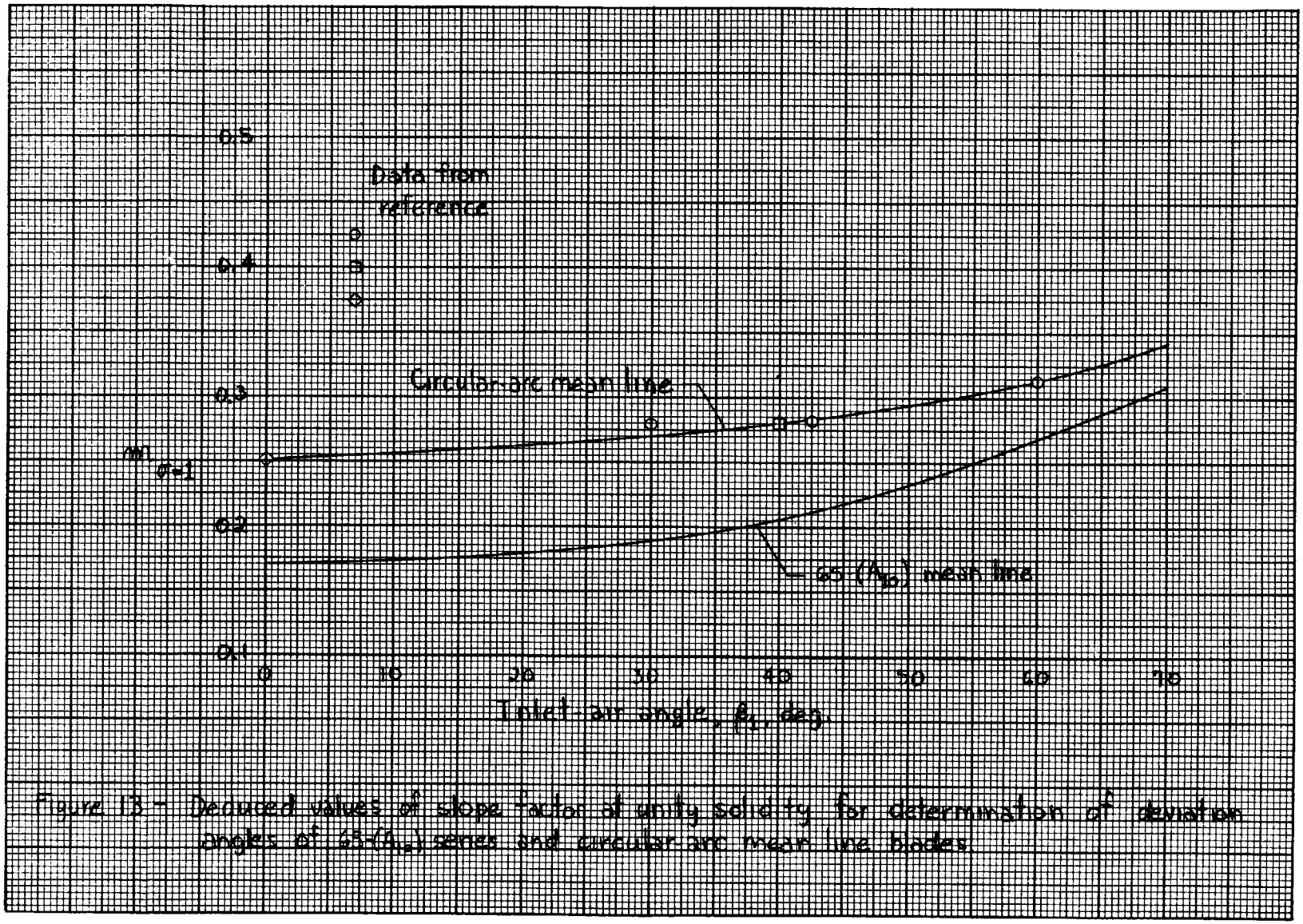

Figure 13 - Deduced values of slope factor at unity solidity for determination of deviation angles of 65-(A_{10}) series and circular-arc mean line blades.

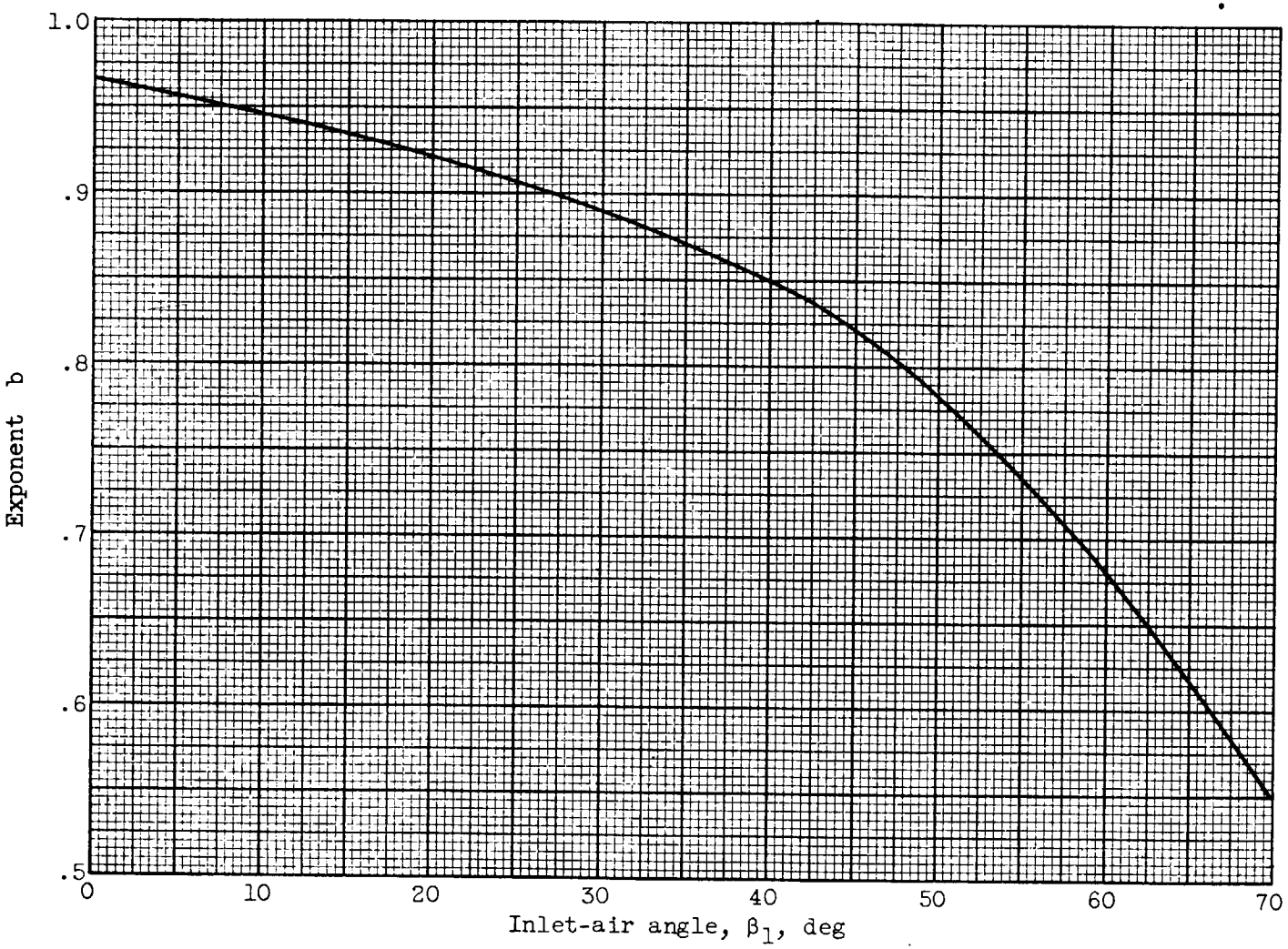

Figure 14. - Value of solidity exponent b in deviation-angle rule (deduced from data for 65-(A_{10})-series blades [6].

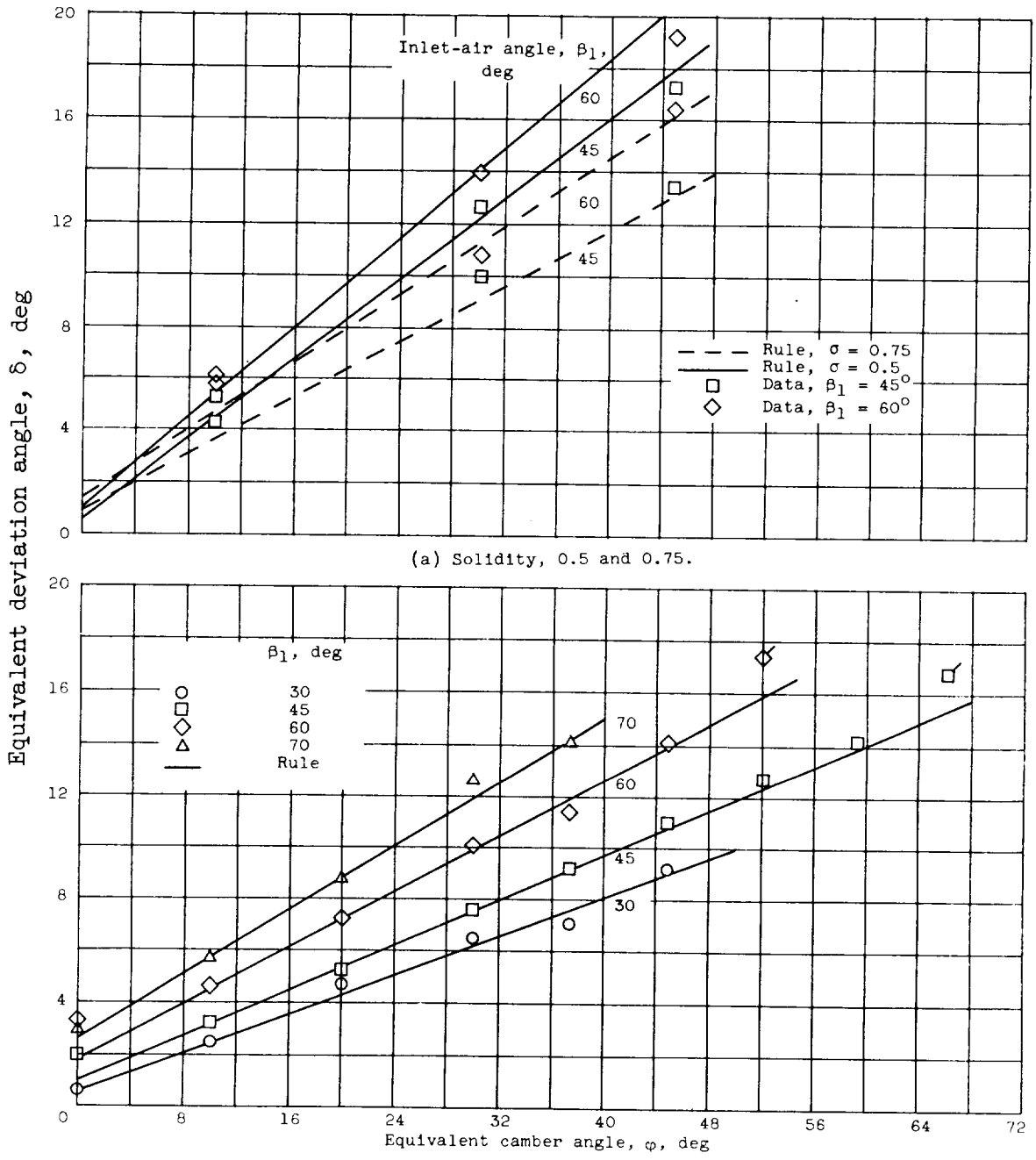

(a) Solidity, 0.5 and 0.75.

(b) Solidity, 1.0.

Figure 15. - Comparison between data values and deduced rule values of reference minimum-loss deviation angle for NACA 65-(A_{10})10-series blades as equivalent circular arcs (data from [6]).

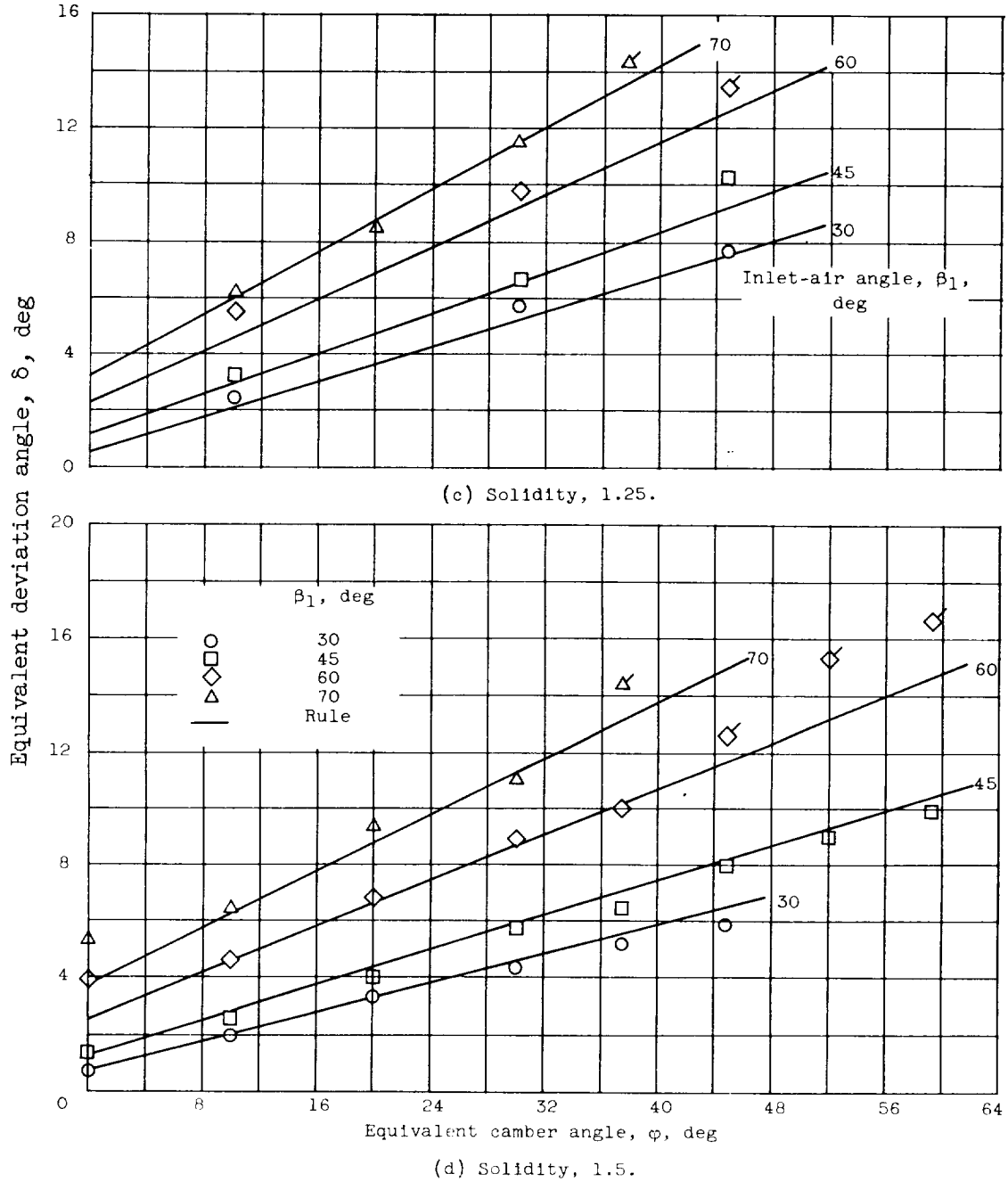

Figure 15. - Concluded. Comparison between data values and deduced rule values of reference minimum-loss deviation angle for NACA 65-(A_{10})10-series blades as equivalent circular arcs (data from [6]).

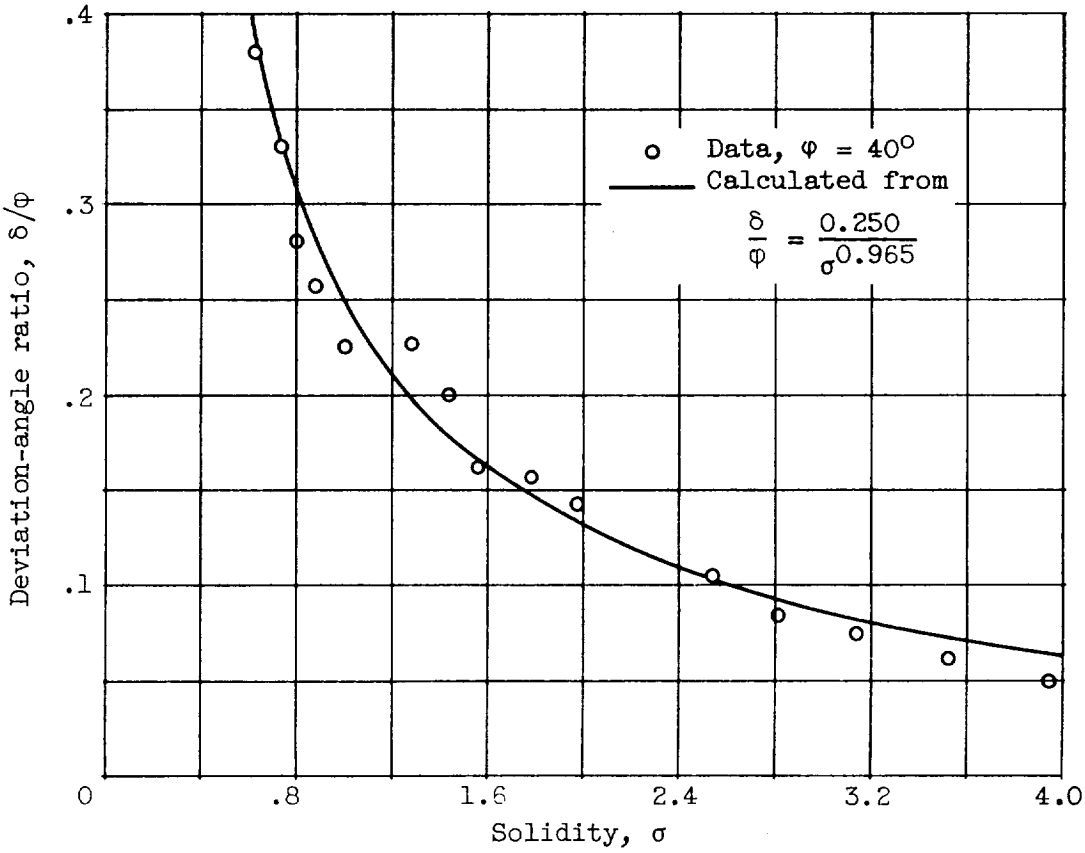

Figure 16. - Comparison of experimental deviation-angle ratio and rule values using solidity exponent given by figure 14. Data for circular-arc inlet guide vanes in annular cascade [27].

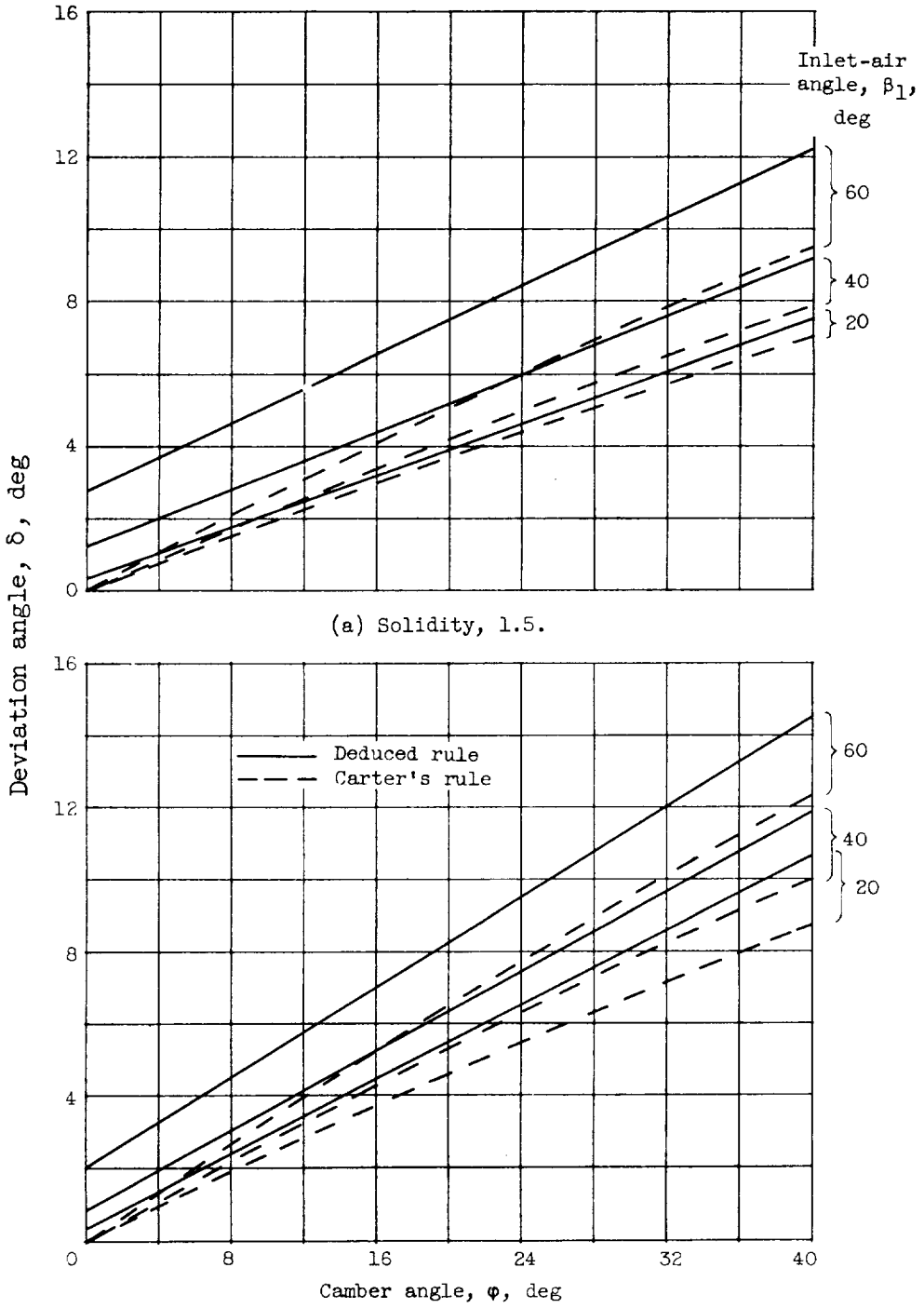

(a) Solidity, 1.5.

(b) Solidity, 1.0.

Figure 17. - Comparison of calculated reference deviation angles according to Carter's rule and deduced modified rule for 10-percent-thick, thick-nose circular-arc blades.

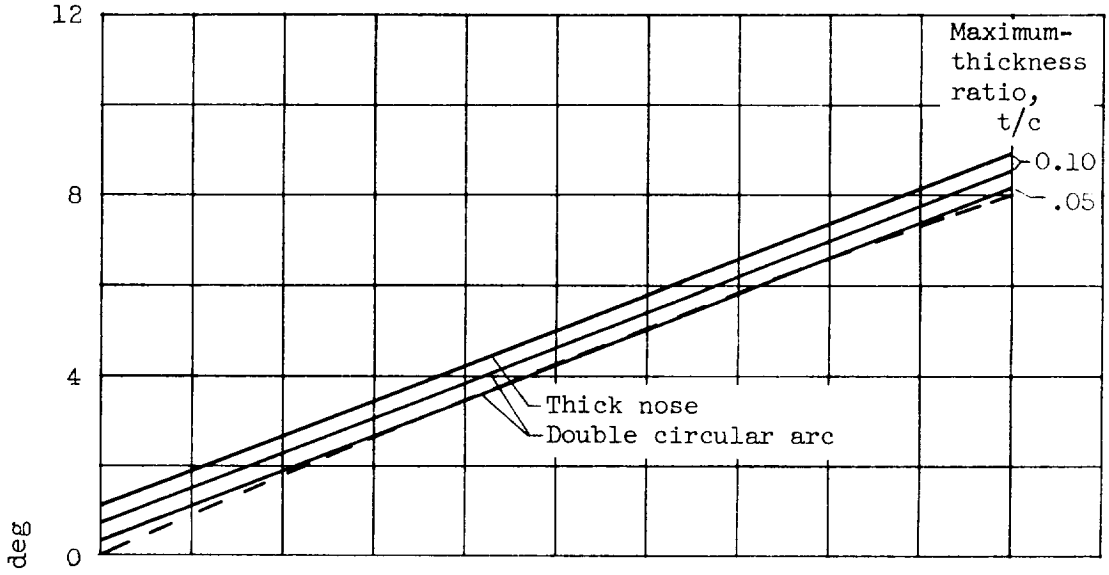

(a) Solidity, 1.5; inlet-air angle, 40°.

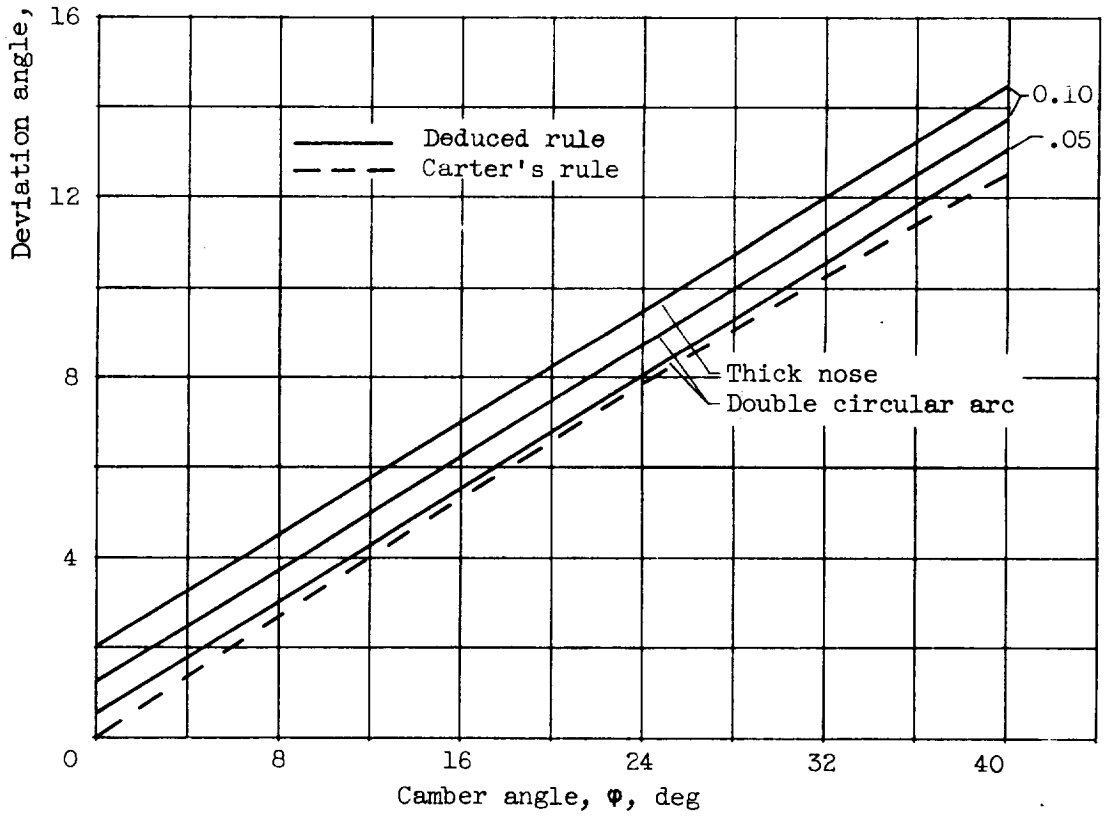

(b) Solidity, 1.0; inlet-air angle, 60°.

Figure 18. - Comparison of calculated reference deviation angles according to Carter's rule and deduced modified rule for circular-arc blades of different thickness.

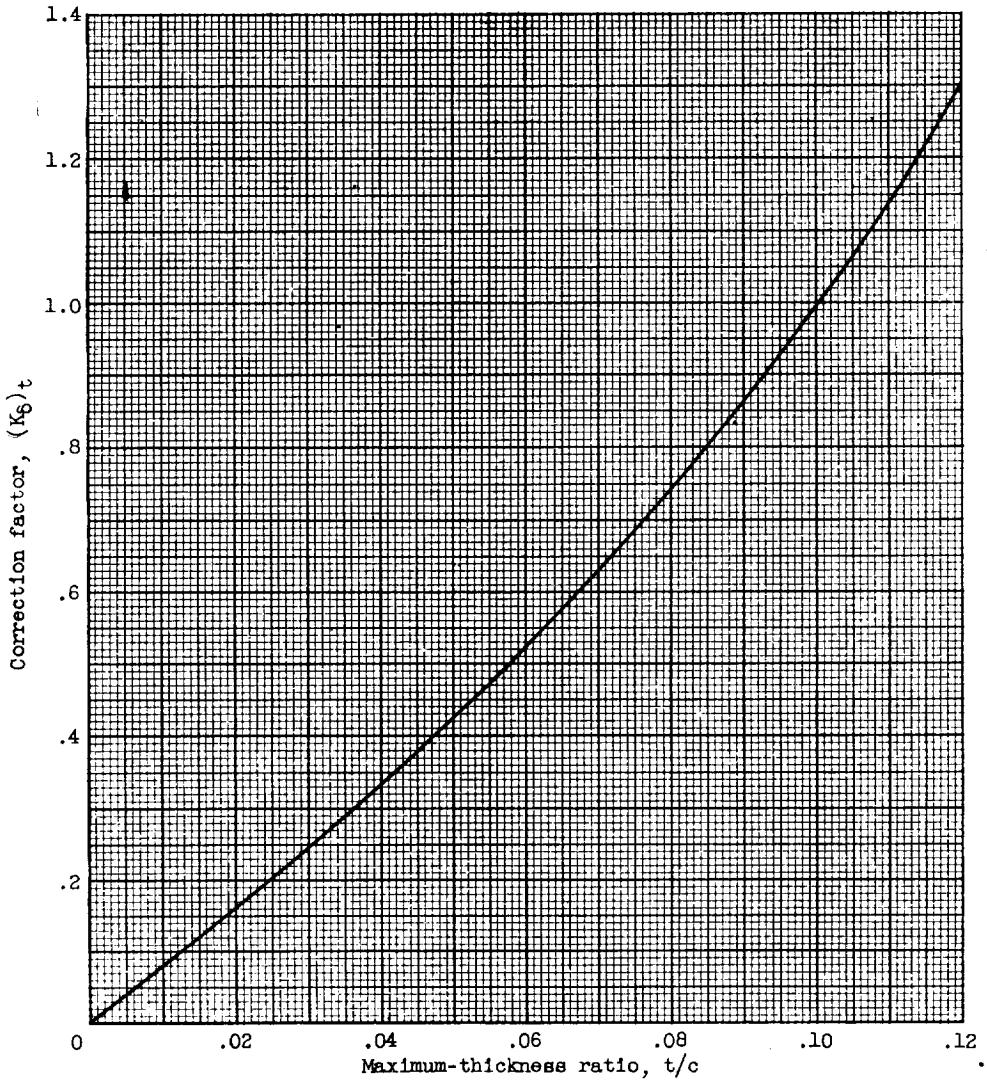

Figure 19. - Deduced maximum-thickness correction for zero-camber reference minimum-loss deviation angle (eq. (13)).

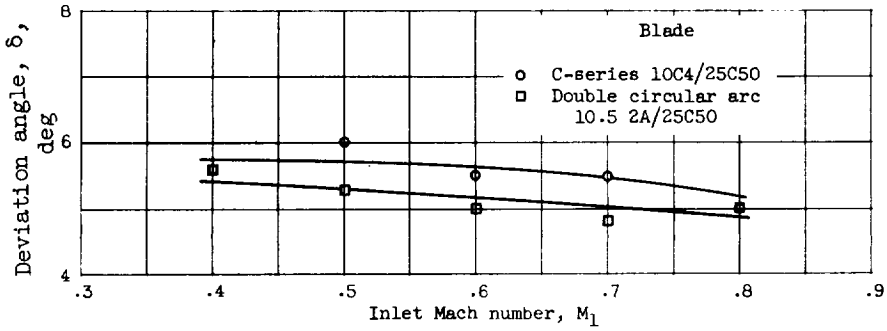

Figure 20. - Variation of reference deviation angle with inlet Mach number for circular-arc blades. Solidity, 1.333; blade-chord angle, 42.5° [12].

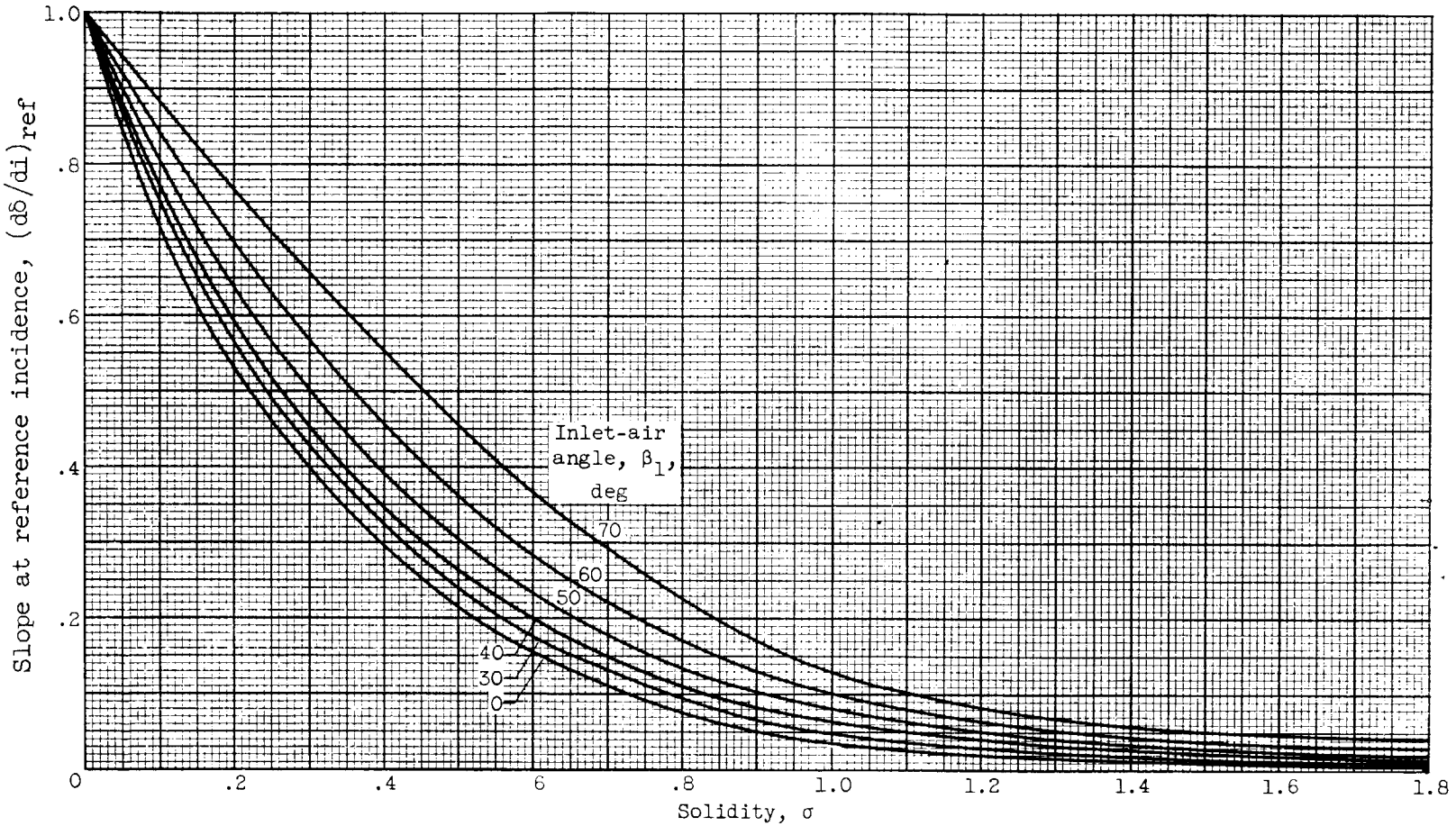

Figure 21. - Deviation-angle slope $d\delta/di$ at reference incidence angle deduced from low-speed data for NACA 65-(A_{10})10 blades [6].